

Accounts

Preparation and Kinetic Stabilization of Highly Strained Paracyclophanes

Takashi Tsuji,* Masakazu Ohkita, and Hidetoshi Kawai

Division of Chemistry, Graduate School of Science, Hokkaido University, Kita-ku, Sapporo 060-0810

(Received August 6, 2001)

In this Account we describe the preparation, structures, and properties of the most highly strained paracyclophanes known to date, i.e. [4]- and [1.1]paracyclophanes and their derivatives. The preparation of these cyclophanes has been accomplished through the photochemical valence isomerization of corresponding 1,4-bridged Dewar benzene derivatives. These strained paracyclophanes are prone to polymerize and are not stable enough to isolate: [4]paracyclophane is rapidly consumed even below −100 °C in fluid solution, though it remains intact indefinitely in a frozen organic glass at 77 K, while [1.1]paracyclophane is stable only below −20 °C in solution. By introducing substituents which sterically hinder access to the bridgehead carbon atoms by other reagents, however, one can remarkably stabilize these species kinetically so as to allow the measurement of ^{1}H NMR spectrum of the former and the isolation of the latter as crystals. The ^{1}H NMR spectrum of the [4]paracyclophane strongly support, in conjunction with theoretical calculations, the sustenance of considerable aromaticity despite the extreme bending of its benzene ring. [4]Paracyclophane is so strained that it is thermodynamically less stable than the corresponding Dewar isomer and the thermal conversion of the benzene form to the Dewar form is observed for the first time. A fully unsaturated derivative of [4]paracyclophane is also generated and confirmed to prefer the structure of 1,2,3,4-tetradehydro[4]paracyclophane rather than that of π-bond isomer, bicyclo[4.2.2]deca-1,3,5,7,9-pentaene. The stabilized [1.1]paracyclophane is found to undergo efficient photochemical transformation into a benzene *p*,*p*′-dimer structure, from which the former is thermally regenerated upon mild heating. Structural characteristic features of the [1.1]paracyclophane and the benzene *p*,*p*′-dimer are revealed by X-ray crystallography. Limits for experimentally accessible strained paracyclophane are also discussed.

Benzene prefers a planar configuration. When bridged with a side chain at the para positions, however, the benzene ring is forced to bend into a boat form unless the bridging chain is sufficiently long. In the past thirty years, the research on the preparation of 1,4-bridged benzene derivatives, i.e. paracyclophanes, with ever shorter bridges has made remarkable progress, driven by the interest in the properties of strained molecules as well as by the challenges inherent in their synthesis and also in the pursuit of improved understanding of aromaticity. Recent developments in the chemistry of small and strained cyclophanes have been summarized in several reviews.[1] In this Account, the results of our research on the preparation, structures, and properties of the most highly strained paracylophanes known to date, i.e. [4]- and [1.1]paracyclophanes and their derivatives, are described.[2]

Flat and rigid was a general view of aromatic hydrocarbons decades ago and the successive preparations of highly distorted [7]paracyclophanes by Allinger[3a] and of [6]paracylophanes by Jones and co-workers[4a] as stable, isolable entities in the early 70's were greeted with great surprise. [6]Paracylophane had remained as the most strained paracyclophane for years until the generation of [5]paracyclophane was confirmed by ^{1}H NMR spectroscopy in 1985 through the collaboration of Bickelhaupt, Tobe, and their co-workers.[5a] A mere three years later, Bickelhaupt et al. found that 1,4-tetramethylene-bridged Dewar benzene underwent the addition of protic solvent molecules to the bridgehead positions under irradiation, accompanied by the cleavage of the central σ bond, and they proposed the generation of [4]paracyclophane as a transient species.[6] At about the same time, we independently made similar observations during the study of photo-induced electron transfer reaction of Dewar benzene derivatives and we subsequently succeeded in measuring the electronic absorption spectrum of [4]paracyclophane and confirming its generation.[7] On the other hand, [2.2]paracyclophane was first isolated in 1949 from the pyrolysate of *p*-xylene.[8] Its structure, in which benzene rings are bent and aligned in parallel in close proximity, has fascinated chemists. Despite the ensuing extensive study on the chemistry of cyclophanes, the lower [1.2] and [1.1] homologues had long remained unknown. During the study on the photochemical generation of [4]paracyclophanes, we realized that [1.1]paracyclophane might well be produced by photochemical isomerization of the corresponding bis(Dewar benzene) derivative, and we subsequently succeeded in the genera-

tion of [1.1]paracyclophane and its derivatives as metastable species[9] and then isolated a kinetically stabilized one[10] as described in this account.

The generation of [4]- and [1.1]paracyclophanes accomplished so far depends exclusively on the photochemical valence isomerization of 1,4-bridged Dewar benzenes. This methodology combines the following favorable aspects: (i) Dewar benzene is a bent isomer of benzene and the Dewar benzene precursors of small cyclophanes are not particularly strained and relatively readily accessible, (ii) the aromatization of Dewar benzene is a highly exothermic process and even the large strain energy of extremely distorted [4]paracyclophane is largely or more than compensated by the aromatization energy in its generation from the Dewar isomer, and (iii) the photochemical aromatization of Dewar benzene is generally devoid of any complicating rearrangement.

1. [4]PARACYCLOPHANE SYSTEM

1.1 [4]Paracyclophanes (Generation and Chemical Trapping) Bickelhaupt and co-workers found that photolysis of **1a** in methanol and in CF_3CO_2H–THF led to the formation of **3a** and **3b**, respectively, and they proposed the intermediacy of [4]paracyclophane (**2a**).[6] We also observed that **1a–c** underwent the addition of alcohols to give **3–3″** under irradiation (Scheme 1).[7] The addition reaction is subject to catalysis by acid and the yields of **3–3″** are substantially increased in the presence of catalytic amounts of trifluoroacetic acid. Those adducts indeed results from the electrophilic addition of the reagents to transient **2a–c** as demonstrated by experiments described later. Because the protonation of [4]paracyclophane at the bridgehead carbon atom leads to an unfavorable bridgehead carbonium ion, the acid-catalyzed addition of alcohol to **2** may proceed more or less concertedly.

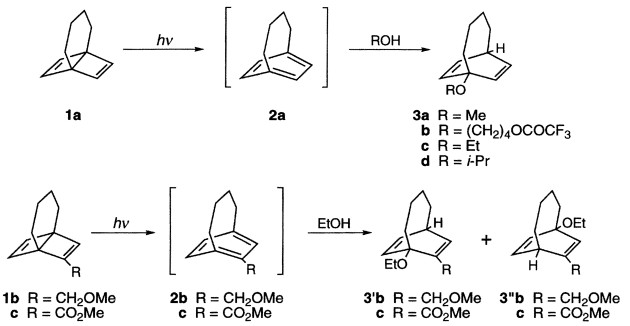

Scheme 1.

(Electronic Absorption Spectra) Compound **1a** exhibits only a weak end absorption extending to ca. 270 nm in the ultraviolet region. Irradiation of **1a** in a glassy mixture of EPA (ether : pentane : ethanol = 5 : 5 : 2) frozen at 77 K with a low-pressure mercury lamp (254 nm) gives rise to the formation of species showing an electronic absorption extending over 400 nm (Fig. 1A).[7] The development of similar absorption is also observed in pentane–isopentane (1 : 1) or in ethanol. The generated species that was later confirmed to be **2a** is indefinitely stable under the matrix isolation in the dark at 77 K, but extremely labile in fluid solution even below −100 °C. The species is also photochemically reactive and, when the resulting

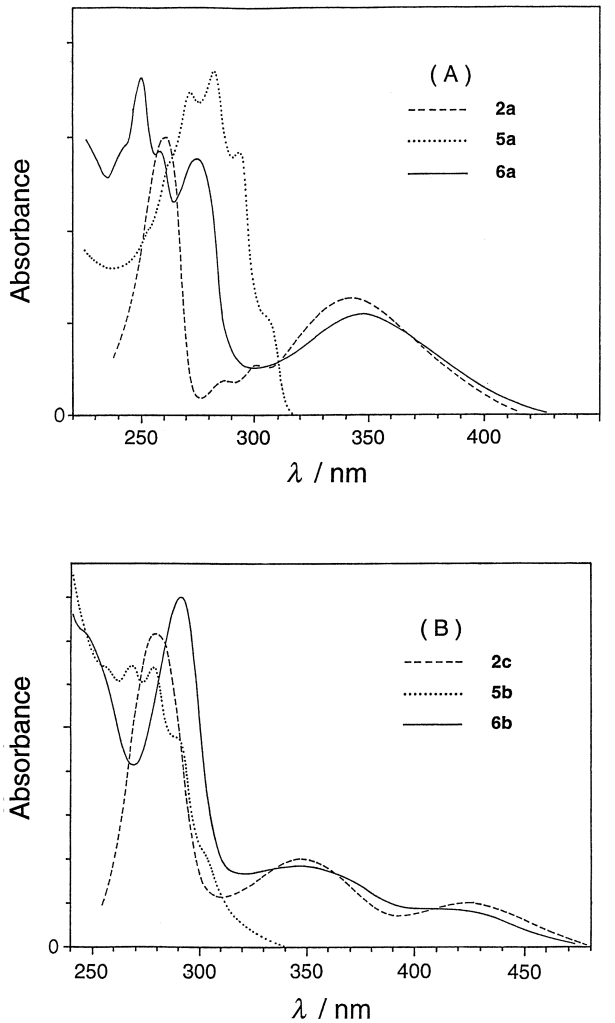

Fig. 1. Electronic absorption spectra (A) of **2a**, **5a**, and **6a**, and (B) of **2c**, **5b**, and **6b** in EPA at 77 K. Relative absorption intensities of the spectra are arbitrary.

mixture at 77 K is irradiated with filtered light (365 nm) with which only the produced **2a** but not **1a** is electronically excited, the developed absorption quickly decays. The difference spectrum obtained from the spectra before and after the secondary irradiation suggests the quantitative reversion of the transient species to **1a**. The ready photochemical valence isomerizations of [5]- and [6]paracyclophanes to the corresponding Dewar benzenes are well documented.[1a–d] Irradiation of **1b** and **1c** in glassy mixtures with 254 nm light at 77 K similarly leads to the formation of **2b** and **2c**, respectively (Fig. 1B). Both the species are photochemically susceptible and can be efficiently converted into the starting Dewar benzenes upon secondary irradiation of the photolyzed glasses with 365 nm light.

When a fluid solution of **1a** in pentane-isopentane was irradiated with a 254 nm light source below −120 °C, the solution turned cloudy and a colorless amorphous precipitate was soon formed; no volatile product was detected in the photolysate. Thus, [4]paracyclophane (**2a**) appears to be extremely prone to polymerization.

(Structural Characterization) The results of the chemi-

cal trapping experiments and of the spectroscopic investigation at low temperature strongly support the transient generation of [4]paracyclophanes from the corresponding Dewar benzene isomers. It is still difficult, however, to rigorously rule out the possibilities that the trapping products were directly derived from the Dewar benzenes in electronically excited states and that the observed absorption spectra were accidentally due to unknown unstable by-products. Fortunately, the generation of the species, thought to be **2**, is photochemically reversible and this reversibility was exploited to obtain more convincing evidence for the structural assignment.

Compound **1a** is stable in ethanol containing 1% (v/v) sulfuric acid; irradiation of a glassy solution of this acidic mixture at 77 K with 254 nm light leads to the development of the same absorption as observed in neutral ethanol. Since **2a** undergoes slow photolysis to give *p*-xylylene and ethylene, as described in the following section, the irradiation was discontinued while the extent of the secondary photolysis remained still insignificant. The resultant mixture was warmed to room temperature to allow the generated species to react with ethanol. If the sulfuric acid is omitted, polymer is predominantly produced. Because the amount of **2a** produced in one freeze–irradiation–thaw cycle was minuscule, the cycle was repeated ten times before the photolysate was analyzed by GC and GC-MS spectrometry. The formation of **3c** under the above conditions was thus confirmed. In the second experiment, the absorption developed by the initial irradiation of 254 nm light was bleached with a secondary irradiation of 365 nm light each time before the glassy mixture was thawed. After having repeated the freeze-irradiation (254 nm)–irradiation (365 nm)–thaw cycle ten times, we analyzed the resulting mixture as before. The amount of **3c** produced in the latter experiment was less than one-tenth of that obtained in the former photolysis. Because **3c** is transparent above 300 nm and hence inert toward 365 nm light, the greatly diminished yield of **3c** in the latter experiment unequivocally demonstrates that **3c** was produced predominantly, if not exclusively, during the thaw in the dark, but not during the irradiation with 254 nm light, and that the precursor of **3c** was quenched by 365 nm light. Thus, the species exhibiting the absorption extending to 420 nm is certainly the direct precursor of **3c**, and **2a** is the only conceivable intermediate capable of accommodating all of the observations. The possibility that **3c** is produced by the addition of ethanol to **1a** in the excited state or to the corresponding prismane intermediate is definitely ruled out. Thus, it is concluded that the electronic absorption spectra developed upon irradiation of **1a–c** at 77 K are due to **2a–c**, from which the adducts **3–3″** are derived.

(Photochemical Reactivity) When **1a** is irradiated with a 254 nm light source at 77 K, a quasi-photoequilibrium between **1a** and **2a** is reached after a short period of time and the absorption due to **2a** ceases to grow. Continued irradiation induces the growth of a new band with a fine structure in the 270–310 nm range. The similarity of the shape of the band to that reported for *p*-quinodimethane (**4**)[11] suggested that secondary photolysis of **2a** gave **4** and ethylene (Scheme 2).[7] Treatment of the photolysate of **1a** in pentane-isopentane with bromine, followed by GC-MS analysis of the product mixture, proved the formation of *p*-bis(bromomethyl)benzene. The delayed development of the absorption due to **4** as compared to that due to **2a** is in accord with its derivation from **2a** via the secondary photolysis rather than directly from **1a**. This type of photodecomposition, however, is not observed for **2c** and the photochemical interconversion between **1c** and **2c** is clean and quantitative under the matrix isolation at 77 K. The photochemical isomerization of **2c** to **1c** may be so efficient that the potential cleavage of the former into ethylene and the 1,4-phenylenebis(methylene) derivative may be overshadowed. Another possibility is that the fragmentation of **2a** into **4** and ethylene may actually take place in vibrationally excited states during the decay from the electronically excited state to the ground state and that the excess vibrational energy may be dissipated much more efficiently in the substituted **2c** than in **2a**.

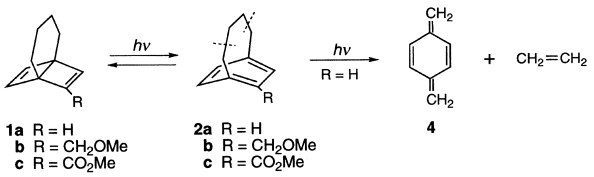

Scheme 2.

(Computational Analysis) Owing to extreme instability, none of the structures of [4]paracyclophane and its derivatives, including the kinetically stabilized one whose preparation is described later, has been experimentally elucidated. A theoretical study of [4]paracyclophane using the minimum basis set and the semiempirical Hamiltonian has been reported by Bickelhaupt and co-workers.[12] More recently, detailed theoretical studies on the structures and properties of **2a** and its valence isomers have been carried out by two groups, Grimme[13] and Schaefer et al.[14]

Table 1 displays selected geometrical parameters that have been calculated for **2a**; for comparison purposes, data for [5]- and [6]paracyclophanes are also listed. The differences between the calculated geometries of **2a** are generally small (bond length < 0.03 Å) and the critical bending angles α and β are $29.7 \pm 0.3°$and $38.9 \pm 0.9°$, respectively. The extent of bond alternation in the benzene ring is less than 0.02 Å at both the SCF and MP2 levels and using the density functional (DFT) method, and thus surprisingly small for the extreme distortion of the ring. The semiempirical method predicts a much larger difference, $\Delta r = 0.034$ Å (MNDO). Compared to the ab initio calculations, the semiempirical methods tend to increase α at the expense of β. It has been pointed out that the overestimation of α in small cyclophanes is a common failure of semiempirical MO and force field methods.[13] As can be seen from the large bond distances and bending angles, a significant amount of strain is placed in the tetramethylene chain (Fig. 2).

Relative energies that have been computed for **1a** and its valence isomers are collected in Table 2. Dewar benzene is so strained and its isomerization to benzene is so exothermic that benzene even in its electronically excited state is thermally populated from the former.[15] The strain energy of paracyclophane, however, is rapidly accumulated as the number of bridging carbon atoms decreases from eight to four, whereas the strain energies of the corresponding 1,4-bridged Dewar benzenes remain virtually unaffected. Thus, the relative ener-

Table 1. Calculated Geometrical Parameters for [*n*]Paracyclophanes (n = 4–6)[13,14,16]

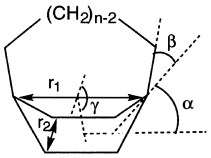

Method	α/deg	β/deg	$(\alpha+\beta)$/deg	γ/deg	r_1/Å	r_2/Å
		[4]Paracyclophane (**2a**)				
SCF/DZP	29.7	38.2	67.9	34.1	2.657	2.374
SCF/TZ2P	29.7	38.0	67.7		2.647	
MP2/DZ+d	29.4	39.7	69.1		2.707	
B3LYP/DZ+d	30.0	38.8	68.8		2.696	
		[5]Paracyclophane				
SCF/6-31G	23.5	28.7	52.2	27.2	2.710	2.385
		[6]Paracyclophane				
SCF/6-31G	18.8	20.0	38.8	22.0	2.750	2.381

Table 2. Calculated Energy Differences of [4]Paracyclophane and its Valence Isomers (in kcal mol^{-1})[a), 13,14]

Method	[4]Paracyclophane (**2a**)	Dewar form **1a**	Prismane form
SCF/DZP	18.3 (17.7)	0	39.2
MP2/DZ+d	3.5 (2.9)	0	38.0
B3LYP/DZ+d	2.2 (1.6)	0	
TCSCF/CISD+Q/DZ+d[b)]	9.9 (9.3)	0	

a) Values after correction for the zero-point vibrational energy differences are given in parentheses. b) Single point energy at the TCSCF/DZ+d optimized geometry.

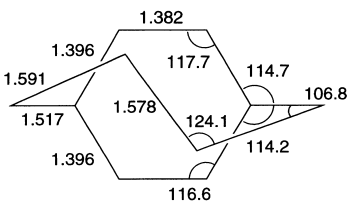

Fig. 2. SCF/DZP optimized structure of [4]paracyclophane (bond lengths in angstroms and bond angles in degrees).

gy of a paracyclophane to its Dewar benzene form is expected to reverse at a certain chain length. In the pentamethylene-bridged derivatives, the benzene form is still lower in energy than the Dewar form.[1,16] Calculations at the SCF/DZP level, however, predict that the relative stability is reversed when the bridging chain is shortened to tetramethylene; **2a** lies ca. 18 kcal mol^{-1} higher in energy than **1a**.[13] The energy difference diminishes at the higher levels of theory, but **2a** is still predicted to lie 2–10 kcal mol^{-1} higher in energy than **1a**(1 cal $\approx$ 4.18 J). As described later, thermal isomerization of bent benzene ring into a Dewar form has been observed for the first time in a kinetically stabilized [4]paracyclophane derivative,[17] in agreement with the theoretically predicted reversal of the relative stability.

The total strain energy for **2a** has been evaluated using the homodesmotic reaction of Eq. 1.[14] The strain energy obtained from the reaction of Eq. 1 is 109.5 kcal mol^{-1} at the SCF/DZP level and 85 kcal mol^{-1} at the MP2/DZP level. A comparable value of 92.7 kcal mol^{-1} is obtained by the

$$C_6H_4(CH_2)_4\ (\mathbf{2a}) + 5\ C_2H_6 \rightarrow p\text{-}(CH_3)_2C_6H_4 + 4\ C_3H_8 \quad (1)$$

semiempirical AM1 method.[18] The total strain energy for **2a** may be partitioned into two parts, one being the strain energy due to the distortion of benzene ring and the other being the strain energy due to the distortion of bridging chain. The former is commonly evaluated as follows: freezing the benzene ring in the conformation present in **2a** and placing the two hydrogens at a typical C–H distance in the same direction as the first carbon atoms of the chain; the energy difference between the above structure and normal planar benzene gives a measure of the strain energy resulting from the distortion of the benzene ring. The analogous calculation for the methylene chain provides the strain energy due to the bridging chain. The results are summarized in Table 3. The total strain energy for **2a** thus evaluated is 107.6 kcal mol^{-1} at the SCF/DZP level and 91.3 kcal mol^{-1} at the MP2/DZP level, in good agreement with the values evaluated by using the reaction of Eq. 1. Evidently the steric strain in **2a** largely arises from the distortion

Table 3. Partitioning of Strain Energy of [4]Paracyclophane (in kcal mol^{-1})[13,14]

Theoretical level	*SE* (C_6H_6)	*SE* (chain)	*SE* (total)
SCF/DZP	95.5	12.1	107.6
MP2/DZP	79.4	11.9	91.3

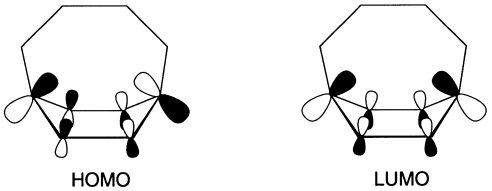

Fig. 3. Schematic description of the HOMO and LUMO of [4]paracyclophane.

of the benzene moiety.

As depicted in Fig. 3, both the HOMO and LUMO of **2a** are essentially centered at the bridgehead positions and, according to CAS-SCF calculations, the HOMO of **2a** formally has a deficiency of 0.23 electrons which are moved mainly into the LUMO, consistent with the diradicaloid nature of **2a.**

1.2 1,2,3,4-Tetradehydro[4]paracyclophane (π-Bond Isomerism in Bicyclo[4.2.2]decapentaene) The successful generation of [4]paracyclophanes **2** from the Dewar isomers **1** suggests that 1,2,3,4-tetradehydro[4]paracyclophane (**6a**) may be accessible via the valence isomerization of 1,3-butadiene-bridged Dewar benzene **5a**. Compound **6a** is a fully unsaturated species and π-bond isomerism in it leads to bicyclo-[4.2.2]deca-1,3,5,7,9-pentaene (**7a**). It is of special interest to determine whether the species resulting from the isomerization of **5** will exist as **6** and/or **7** or conceivably some structure of lower symmetry (Scheme 3). The paracyclophane structure **6a** is expected to be no less strained than **2a**, due to the rigidity of the bridging chain, and hence no less reactive. On the other hand, the decapentaene structure **7a** may be viewed as a 1,6-etheno-bridged cyclooctatetraene in which the bridgehead double bonds are constrained to interact through space and there may also be through-bond interaction. The related compounds, anti-Bredt dienes **8** and **9**, have been prepared by Wiseman[19] and Wiberg,[20] respectively. Of particular interest is the property of **10** reported by Greene et al. (Scheme 4)[21] Compound **10** is stable to heat, acid, and moisture, despite the severe out-of-plane bending at the olefinic carbons. It appears that the steric strain in **7** is more evenly distributed over the skeleton than in **6** and the former may be superior in kinetic stability to the latter. As described in the following sections, the species photochemically generated from **5a,b** possess the structures of **6a,b**, respectively, in preference to those of **7a,b** and are as labile as the corresponding [4]paracyclophanes.[22]

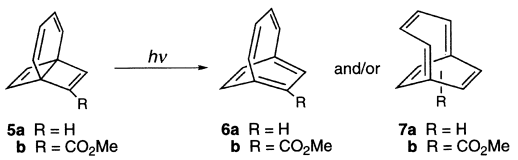

Scheme 3.

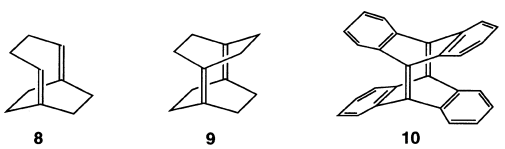

Scheme 4.

(Preparation of the Dewar Benzene Precursors) Synthesis of [4.2.2]propellatetraenes **5**, the Dewar benzene precursors for **6/7**, was achieved as outlined in Scheme 3,[22,23] namely, the photocycloaddition of dichloroethylene to dihydroindanone **13** followed by the reductive elimination of chlorine, and the diazotization and photo-Wolff ring contraction of the cyclopentanone moiety to afford **18**. The bromination of **18** exclusively occurred at the cyclohexene double bond and subsequent dehydrobromination delivered **19**, from which **5b** was obtained following the selenenylation-oxidation-elimination protocol.[24] The preparation of parent **5a** was accomplished via a reaction sequence in which **19** was converted successively into the carbamate,[25] amine, quaternary ammonium salt, and the tetraene (Scheme 5).

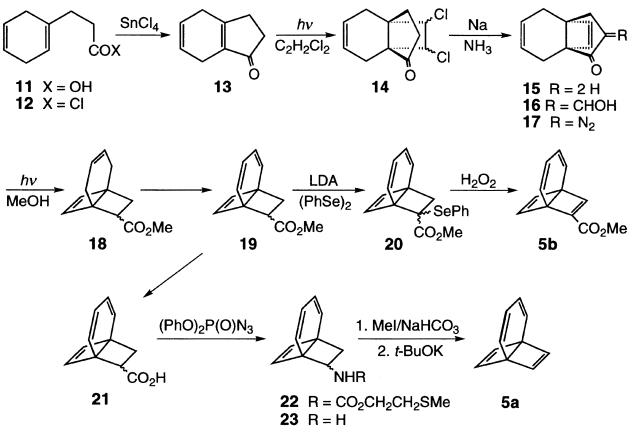

Scheme 5.

Electronic interaction among the three π-bond systems in **5** is of considerable interest. Photoelectron spectroscopic study, however, reveals that the interaction is rather weak at least in the ground state.[26]

(Chemical Trapping Experiments) The chemical trapping of transient *anti*-Bredt bridgehead olefins with reactive conjugated dienes as Diels-Alder adducts is a well established technique and provides reliable verification for their generation.[27] This method, however, could not be applied for the trapping of **2** because the photolysis of the Dewar benzene precursors **1** in the presence of conjugated diene was impractical, owing to the preferential absorption of incident light by the latter rather than the former. Fortunately, the electronic absorptions of **5a,b** extend to wavelengths substantially longer than that of cyclopentadiene, enabling the selective excitation of the former in the presence of the latter. Irradiation of a mixture of **5a** and a large excess of cyclopentadiene in hexane through Pyrex cleanly affords two 2 : 1 adducts of cyclopentadiene to **5a** in a ratio of ca. 2 : 1, for which the structures **24** and **25**, respectively, are assigned (Scheme 6). The strong electronic absorptions in the region of 250–300 nm exhibited by these products substantiate the presence of a conjugated diene unit and effectively rule out their derivation from **7a**. Products resulting from the addition of cyclopentadiene to **7a** at the bridgehead double bonds should only possess isolated double bonds. Virtually no volatile product other than **24** and **25** is detected in the photolysate. The preferential trapping of the decapentaene in the form of [4]paracyclophadiene **6a** was thus confirmed.

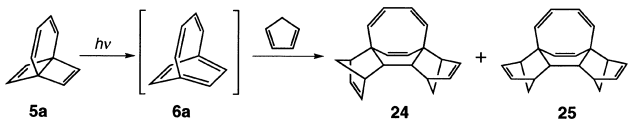

Scheme 6.

Photolysis of **5b** in the presence of cyclopentadiene leads to the formation of a rather complex product mixture, from which **26–31** are eventually isolated in 27% yield in total (Scheme 7 and 8). The products **29–31** apparently result from the addition of cyclopentadiene to the substituted side of the bent benzene ring of **6b** and, interestingly, have suffered secondary (photo)rearrangement. As illustrated in Scheme 8, their formation is rationalized in terms of the secondary di-π-methane rearrangement[28] and [2 + 4] addition in the initial adduct(s) **32**, possibly facilitated by the accompanying relief of steric congestion. The formation of products which could be derived from **7b** was not observed again.

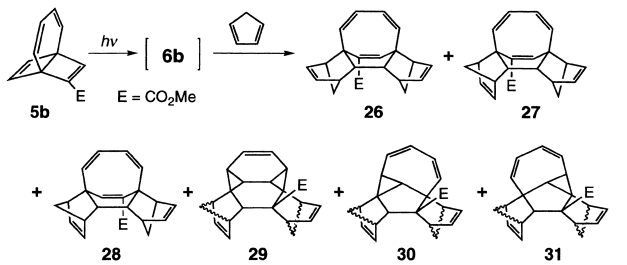

Scheme 7.

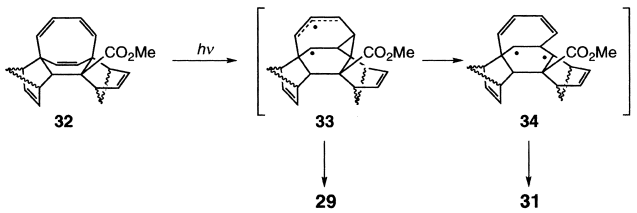

Scheme 8.

(Electronic Absorption Spectra) In addition to the aforementioned trapping experiments, a spectroscopic study also supports the preferential formation of bicyclo[4.2.2]decapentaene in the form of **6** rather than **7**. Thus, irradiation of **5a** in an EPA glass with a low-pressure mercury lamp at 77 K gives rise to an electronic absorption showing λ_{max} at 274 and 347 nm (Fig. 1A). The generated species is indefinitely stable under matrix isolation at 77 K in the dark, but undergoes complete decomposition when the glass is thawed below −120 °C. The species is also photochemically susceptible and, upon secondary irradiation with 365 nm light with which only the transient is excited, the developed absorption is efficiently bleached to restore the original spectrum of **5a**. This photochemical behavior is reminiscent of [4]paracyclophane (**2a**) and suggests that the intermediate photochemically reverts to **5a**. Irradiation of **5b** also leads to a species which exhibits a UV-visible spectrum shown in Fig. 1B and whose thermal and photochemical behavior is similar to that observed for the product from **5a**.

The similarity in shape of the observed spectra to the spectral shapes of the corresponding [4]paracyclophanes **2a,c** is striking. In **6**, the π bond system in the four carbon bridge and that of the bent benzene ring are nearly orthogonal to each other, and there will be little interaction between them. If the species generated from **5a,b** have the structures of **7a,b**, respectively, the observed spectra will be much different from those of **2a,c**. In **7**, the neighboring π bonds overlap with each other only weakly. Such a poorly conjugated system tends to exhibit a broad, weak absorption spectrum.[29] Cyclooctatetraene is a notable example,[30] and the π bond system of **7** may be viewed as that of cyclooctatetraene perturbed by the etheno bridge double bond.

On the basis of the regioselective addition of cyclopentadiene and the transient absorption spectra being remarkably similar in shape to those of the corresponding **2**, it is concluded that the irradiation of **5** leads to a species which is best represented by the structure **6**.

(Computational Analysis: 1,2,3,4-Tetradehydro[4]paracyclophane vs Bicyclo[4.2.2]deca-1,3,5,7,9-pentaene) The experimental observations described above unambiguously demonstrate that the reacting species photochemically generated from **5** possesses the structure of **6** rather than that of **7**. Those results, however, do not provide information concerning the latter. To investigate the structures and relative energies of the species **6a** and **7a**, theoretical analyses were carried out by ab initio quantum mechanical methods as well as by semiempirical procedures.[31,32] The geometrical optimizations of bicyclo[4.2.2]decapentaene were undertaken at various levels of theory. An initial exploration of the potential energy surface of the decapentaene with the 3-21G basis set and with semiempirical methods furnished two local energy minima corresponding to the C_{2v} symmetric **6a** and the C_s symmetric **7a**. The optimization of **6a** and **7a** with the 6-31G* basis set were accordingly performed within the constraint of C_{2v} and C_s symmetries, respectively. The selected geometrical parameters for **6a** and **7a** are summarized in Table 4 and Fig. 4.[22b,33]

The most pronounced differences among the structures of **6a** optimized by the ab initio, DFT, and semiempirical methods are found in the deformation angles α and β, as is the case with **2a**. The total deformation angles ($\alpha + \beta$), however, agree within 1.4° (73.9 ± 0.7°) in all the calculations. The aromatic ring is significantly more distorted than that of **2a**, and **6a** represents the most strained of the [n]paracyclophanes prepared to date. As has been pointed out for **2a**, the degree of calculated bond alternation in the benzene ring is remarkably small ($\Delta r <$ 0.02 Å) for such an extremely bent ring. The most notable deformation in the 1,3-butadienylidene bridge is the opening of the C^2–C^3–C^4 angle to about 137° Figure 5A shows torsion angles about the bond between C^1 and C^8 of **6a** and degrees of pyramidalization (out-of-plane bending) at these aromatic carbon atoms.[34] The pyramidalization at the aromatic methine carbon atoms is the consequence of maximization of π-orbital overlap with the adjacent bridgehead carbon atom: otherwise the corresponding π bonds are essentially broken to give rise to the degeneration of **6a** into a biradicaloid.[35] It is instructive that the corresponding unsaturated carbons of **7a** remain virtually planar (out-of-plane bending at $C^{7(8)}$ and $C^{9(10)} < 2.2°$).

Structural parameters for the geometry-optimized C_s form **7a** are also presented in Table 4 and Fig. 4B. A separation be-

Table 4. Comparison of Calculated Geometrical Parameters for the C_{2v} and C_s Forms of Bicyclo[4.2.2]decapentaene[22b,33]

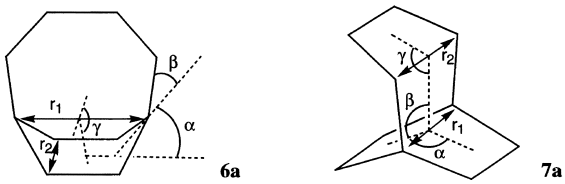

Method	α/deg	β/deg	$(\alpha + \beta)$/deg	γ/deg	r_1/Å	r_2/Å
		C_{2v} Symmetric form **6a**				
SCF/6-31G*	29.0	44.8	73.8	32.5	2.645	2.390
B3LYP/6-31G*	28.0	46.6	74.6	31.8	2.685	2.413
MP2/6-31G*	26.7	47.8	74.5	30.3	2.700	2.420
		C_s Symmetric form **7a**				
SCF/6-31G*	123.8	118.8		131.6	2.400	2.711
B3LYP/6-31G*	124.9	118.4		132.0	2.422	2.738
MP2/6-31G*	125.2	118.2		129.3	2.414	2.680

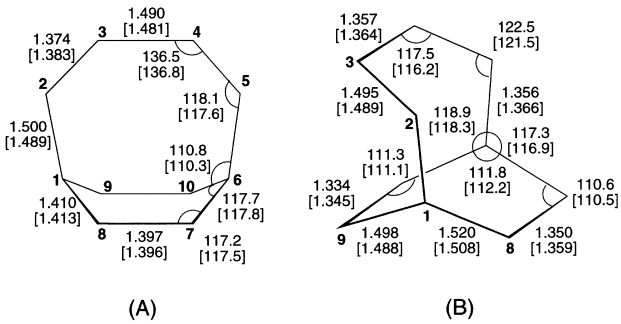

Fig. 4. Calculated molecular structures of **6a** (A) and **7a** (B) optimized at the B3LYP/6-31G* level. Those at the MP2/6-31G* level are given in brackets.

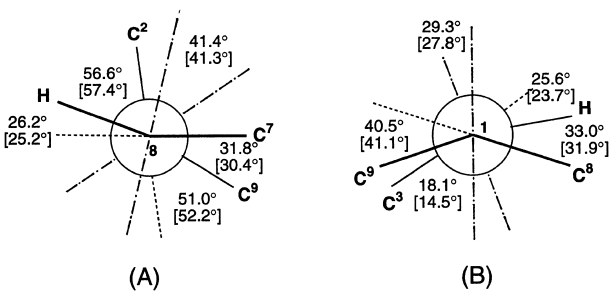

Fig. 5. Newman projections along the C(8)–C(1) bond of **6a** (A) and along the C(1)–C(2) bond of **7a** (B), illustrating geometrical distortions at the strained unsaturated carbon atoms in their B3LYP/6-31G* optimized structures. The corresponding distortions in the MP2/6-31G* structures are given in brackets.

tween the bridgehead carbon atoms, C^1 and C^6, of ca. 2.41 Å suggests that there should be significant interaction between the π electrons of the two bridgehead double bonds. The degrees of torsion about the bridgehead double bond (28–29°) and of pyramidalization at the terminal carbons C^1 and C^2 (ca. 41° and 25°, respectively) are shown in Fig. 5B. These deformation angles are substantially smaller than the corresponding values in **6a**, suggesting the superior kinetic stability of **7a**. The increased HOMO–LUMO energy gap in **7a** (0.445 au vs 0.355 au in **6a** at the SCF/6-31G* level) reinforces the above expectation.

The energy differences between **6a** and **7a**, calculated with ab initio and DFT methods as well as with the semiempirical AM1 method, are listed in Table 5. Inspection of the Table reveals that the semiempirical method as well as the ab initio calculations at the SCF level predict, contrary to the experimental observations, that the C_{2v} form **6a** is less stable than the C_s form **7a**. With the application of the 2nd order Møller–Plesset (MP2) correlation energy treatment or with the DFT method, however, the energy of **6a** is remarkably lowered relative to **7a** and the C_{2v} form is now predicted to lie 4–5 kcal mol^{-1} below the C_s form. Taking the experimental observations into account, it seems safe to conclude that the C_{2v} form is thermodynamically more stable than the C_s form. The predicted energy difference between the two forms, however, is small and it is suggested that the structural preference may be electronically and/or sterically shifted to the C_s form by the introduction of suitable substituents. Strain energies arising from the deformation of the benzene moiety and the butadiene bridge of **6a** were evaluated separately in the same manner as that described for [4]paracyclophane (**2a**). The results are summarized in Table 6.[33]

1.3 Kinetic Stabilization and Aromaticity of [4]Paracyclophane The extreme lability of [4]paracyclophanes seems to arise from the high propensity for undergoing addition at the bridgehead positions, whereby the steric strain inherent to the [4]paracyclophane skeleton is largely relieved. The chemical trapping of **2** with protic reagents indeed resulted regioselectively in the formation of adducts **3–3″** at the bridgehead carbon atoms. The high reactivity at the bridgehead sites may also be rationalized in terms of the HOMO and LUMO, which are essentially centered at these positions. These observations suggest that the [4]paracyclophane system may be kinetically stabilized, to some extent at least, by introducing sterically de-

Table 5. Calculated Energy Difference of **6a** and **7a** (in kcal mol^{-1})[22b,33]

	AM1	SCF/6-31G*	B3LYP/6-31G*	MP2/6-31G*
E (**6a**) − *E* (**7a**)	6.4	8.8	−3.9	−5.2

Table 6. Partitioning of Strain Energy in **6a** (in kcal mol^{-1})[33]

Theoretical level	*SE* (C_6H_6)	*SE* (chain)	*SE* (total)
SCF/6-31G*	104.4	9.3	113.3
B3LYP/6-31G*	92.4	7.7	99.9
MP2/DZP	90.5	9.1	99.6

manding substituents that specifically shield the bridgehead carbon atoms from access by attacking reagents. A molecular modeling study suggested **35–37** as promising candidates and their preparation was next investigated (Scheme 9).

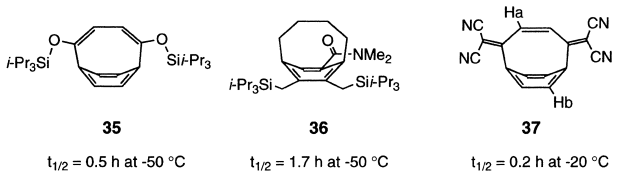

Scheme 9.

(Preparation of the Dewar Benzene Precursors) The preparation of the requisite precursors for **35–37**, namely Dewar benzene derivatives **43**, **44**, and **47**, was carried out as outlined in Schemes 10 and 11.[36] The addition of photochemically generated singlet oxygen to **5a** afforded *endo*-peroxide **38** in an excellent yield, from which **43** and **44** were synthesized following the known procedures. The precursor **47** for **36** was obtained from **46** in essentially the same manner as described for **5b**, and **46** was in turn prepared by the photocycloaddition of **45** to **13**.[37,38] In **37**, the plane containing the exocyclic double bonds bisects the bent aromatic ring, and one of the cyano groups on each terminal carbon atom is disposed near the neighboring bridgehead carbon atom. In **35** and **36**, the bulky substituents are conformationally not fixed, but are expected to effectively shield the bridgehead sites in their preferred conformations.

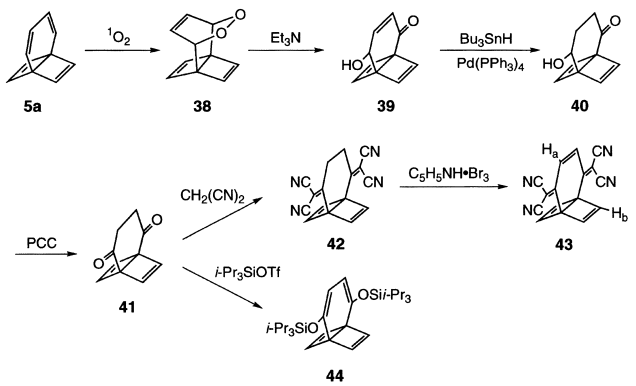

Scheme 10.

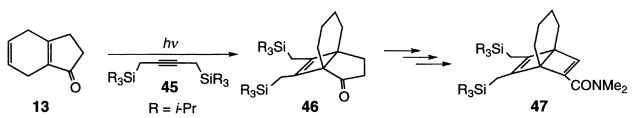

Scheme 11.

(Electronic Absorption Spectra) Irradiation of **43**, **44**, and **47** in ether–isopentane glasses at 77 K with a 254 nm light source invariably leads to the development of bathochromically shifted absorptions. These decay upon subsequent irradiation with filtered light with which only the generated species are excited. This photochemical behavior and the shapes of the absorption spectra suggested the generation of the corresponding [4]paracyclophanes, **35–37**. When the glasses containing the photoproducts were thawed below −100 °C, the absorptions ascribed to **35–37** remained unbleached, in marked contrast to the instantaneous consumption of **2** and **6** in fluid solution even below −120 °C. The half-lives of **35–37** at the specified temperatures are listed in Scheme 9. The highest kinetic stabilization was attained in **37**, and its stability was high enough to permit the measurement of the ^{1}H NMR spectrum. Another hurdle to be cleared in order to measure an NMR spectrum of [4]paracyclophane is its proportion to the Dewar benzene precursor at the photostationary state. Fortunately, the proportion of **37** to **43** at the (quasi)photoequilibrium (365 nm) was sufficiently high to permit the measurement of the ^{1}H NMR spectrum.

(^{1}H NMR Measurement) The ^{1}H NMR spectrum of **43** in CD_2Cl_2 at −90 °C exhibits a pair of singlets at δ 6.93 and 7.20 in a ratio of 2 : 1. Irradiation of **43** with 365 nm light at this temperature leads to the development of a pair of weak singlet signals with an intensity ratio of about 1 : 2 at δ 5.85 and 7.97, respectively; thus the signal of H^a is shifted upfield by 1.35 ppm, whereas that of H^b is shifted downfield by 1.04 ppm upon the transformation of **37** into the product. The intensities of the product signals cease to increase after about 6% conversion. When the resulting mixture is irradiated with light of wavelength longer than 400 nm, the latter pair of signals disappear and the original two line spectrum is restored. Thus the observed changes in the ^{1}H NMR spectra closely correspond with those in the electronic spectra. If the generated species is indeed **37**, the observed chemical shift changes imply the induction of a substantial aromatic ring current despite the extremely bent benzene moiety. For such a conclusion to be drawn, an unambiguous structural assignment should be made to the product. However, the newly developed spectrum was extremely simple and of low relative intensity, and could happen to be due to an unknown side product. Therefore, recourse to computational analysis was made to confirm the structural assignment.

Scheme 12.

Geometrical optimization and calculations of proton chemical shifts were carried out for truncated systems **48–50** (Scheme 12). The results are summarized in Table 7. Calcu-

Table 7. Calculated ^{1}H Chemical Shifts for **48**–**50**[a)]

Compound	$\delta(H^a)$	$\Delta\delta(H^a)$[b)]	$\delta(H^b)$	$\Delta\delta(H^b)$[b)]
48	6.30		6.82	
49	4.82	−1.48	8.38	1.56
50	6.51	0.21	2.72	−4.10

a) GIAO/6-31+G*//B3LYP/6-31G*. b) Chemical shift changes from $\delta(H^a/H^b)$ of **48**. Positive values denote downfield shifts.

lated chemical shifts (GIAO[39]/6-31+G*//B3LYP/6-31G*) are not in particularly good agreement with the experimental values due to the omission of the substituents, but the results are quite instructive. Thus, H^a is predicted to be upfield shifted by 1.34 ppm whereas H^b will be downfield shifted by 1.56 ppm upon the isomerization of **48** to **49**, in good agreement with the experimental observation. The corresponding prismane derivative **50** is apparently incompatible with the observed signals. Because it is expected that the effects of the cyano groups on the chemical shifts are largely compensated in those chemical shift changes, the calculation results provide a strong support to the structure of **37** and suggest the sustenance of relatively strong diatropicity in its aromatic ring despite the extreme bending.

(Aromaticity of [4]Paracyclophane) Aromaticity is a fundamental concept of great importance in organic chemistry, yet unfortunately seems to lack a generally accepted criterion. Recently, Schleyer and co-workers have proposed two probes, as effective aromaticity/antiaromaticity criteria, in which aromaticity is associated with cyclic arrays of mobile electrons with favorable symmetries; namely, diamagnetic susceptibility exaltation (Λ)[40] and nucleus-independent chemical shift (NICS).[41] According to these definitions, significantly exalted (negative) Λ and large negative NICS denote aromaticity whereas positive Λ and NICS denote antiaromaticity. The NICS value is the magnitude of absolute magnetic shielding in ppm, computed e.g., at ring center, and a negative value suggests a diamagnetic ring current effect in the ring. The NICS calculated at the center of the six-membered ring of **49** (GIAO/6-31+G*//B3LYP/6-31G*) is −9.0 while those at the midpoint between the bridgehead carbon atoms and at the center of rectangle formed by the other four aromatic carbon atoms are −11.8 and −7.8, respectively, as compared with −9.7 for planar benzene (Scheme 13). The value of Λ computed for a bent benzene whose geometry is constrained to that present in **49** is −11.6 ppm cgs (CSGT[42]/6-311+G**) as compared with −15.1 ppm cgs reported for planar benzene.[43] The relatively large negative Λ and NICS values, together with the calculated small degree of bond length variation in the six-membered ring of **49**, suggest that **49** and, accordingly, **37** retain relatively good electron delocalization in their bent benzene rings. These experimental and computational results for **37**/**49** are in line with the predictions by Schaefer and co-workers for [4]paracyclophane (**2a**).[14] They have shown in their theoretical study on **2a** that boat-shaped benzene with the same geometry as in **2a** has almost the same magnetic susceptibility, a criterion of aromaticity, as a hypothetical planar cyclohexatriene and a weak ring current is expected in it. It may be relevant to note that benzene can assume localized cyclohexatriene structure with relatively little energy loss.[44]

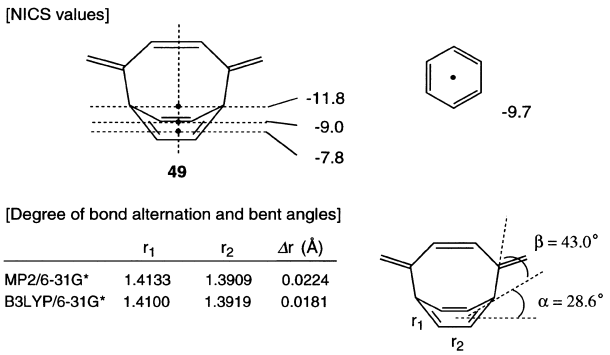

Scheme 13.

On the other hand, the strain energy of [4]paracyclophane (90–100 kcal/mol) mainly arises from the distortion of the benzene ring and far exceeds the resonance stabilization energy of benzene (20–30 kcal/mol).[45] Moreover, [4]paracyclophane and its derivatives behave chemically like activated alkenes and readily undergo addition reactions rather than substitution reactions. Accordingly, they cannot be regarded as aromatics so far as their chemical reactivities are concerned. How can the chemical property of [4]paracyclophane be reconciled with its aromaticity? The sustenance of cyclic delocalization of π-electrons in the severely distorted benzene ring of [4]paracyclophane seems to be a consequence of extensive pyramidalization-rehybridization at the ring carbon atoms to avoid the rupture of the π-bonds leading to the degeneration of [4]paracyclophane into a biradical(oid), and basically not attributable to resonance stabilization effects. In other words, [4]paracyclophane may be stabilized to some extent by the cyclic delocalization of π-electrons, but it maintains the aromatic electron delocalization as the result of the pyramidalization-rehybridization, at the expense of energy much greater than that of resonance stabilization, to accommodate the geometrical constraint imposed on the ring system. Thus, **37** seems to behave like an aromatic as judged by those magnetic criteria of aromaticity, and yet is a kinetically highly reactive, high energy species.

(Benzene vs Dewar Benzene. Reversal of the Relative Stability in [4]Paracyclophane) As described above, theoretical calculations suggest that 1,4-bridged Dewar benzene becomes almost isoenergetic to or slightly lower in energy than the corresponding paracyclophane when the bridging chain is shortened to tetramethylene, $-(CH_2)_4-$. Thus it is suggested that thermal isomerization of [4]paracyclophane to the corresponding Dewar form is at least energetically feasible. The extreme thermal instability of [4]paracyclophane and its derivatives, however, has impeded the observation of their possible thermal transformation into the Dewar forms. The kinetically stabilized **37** is slightly more strained than the parent **2a** and the relative energy calculated for the truncated system, **48**/**49**, suggests that it is not unreasonable to expect the thermal cycloreversion of **37** to **43** to occur, provided that the degree of kinetic stabilization in **37** against its consumption by bimolecular reactions is sufficiently high.[46] The spectral changes observed upon briefly warming a solution of **37** to room tempera-

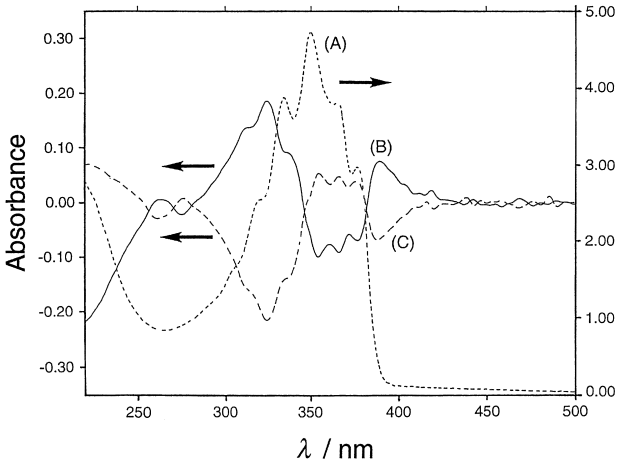

Fig. 6. Electronic absorption spectra in diethyl ether–isopentane (1 : 1) at 77 K: (A) for **43**; (B) as the difference spectrum between those before and after the irradiation of **43** with 365 nm light, and (C) as the difference spectrum between those before and after the subsequent brief heating of the photolyzed mixture to room temperature.

ture corroborated the expectation.[17]

Compound **43** in an ether-isopentane glass at 77 K exhibits a characteristic absorption band with fine structure in the range of 300–390 nm (Fig. 6A). Irradiation of the glassy mixture with 365 nm light leads to the development of absorption due to **37** in the 280–420 nm range at the expense of **43**, as clearly displayed in the difference spectrum (B). When the frozen mixture was thawed, warmed to room temperature, and then refrozen after 1 min in the dark, the resulting difference spectrum (C) between those before and after the heating was a near mirror image to spectrum (B), indicating nearly quantitative thermal reversion of **37** to **43**. The half life of **37** at -20 °C is 15 ± 5 min and, accordingly, the free energy of activation for the isomerization $\Delta G^{\ddagger}$ is 18.3 ± 0.3 kcal mol^{-1} at the same temperature. The agreement of this energy barrier with a recent theoretical value (22 kcal mol^{-1}) for the isomerization of parent **2a** to the Dewar form **1a**[14] is extremely good, especially when a slightly higher exothermicity for the process from **37** to **43** as compared to that from **2a** to **1a** is taken into account.

1.4 Limit for Experimentally Accessible Strained Paracyclophanes The generation of [5]- and [4]paracyclophanes known to date has relied on the photochemical valence isomerization of 1,4-bridged Dewar benzenes. Readers may wonder if the more strained species, e.g. [3]paracyclophane, is experimentally accessible. Our experimental observations suggest that [4]paracyclophanes are near the limit in accessibility, at least by the methodology described above. In contrast to the experimental observations on **1**, **5**, and **43**, no absorption ascribable to **55** is developed upon irradiation of **51** in an EPA glass at 77 K (Scheme 14). Moreover, photolysis of **51** in methanol provides no solvent-incorporated product even in the presence of trifluoroacetic acid. Slow isomerization of **51** to **54** proceeds instead under irradiation. Owing to an additional ethano bridge, the benzene ring in **55**, if it were formed, suffers more severe distortion than those in **2a** and **6a**. According to theoretical calculations at the B3LYP/6-31G* level, the critical bending angles α and β in **55** are 38.0° and 45.5°, respectively, and, thus, the total bending angle ($\alpha + \beta$) amounts to 83.5°, ca. 10° greater than that for **6a**. The photoisomerization of **51** into **54** is significantly slower than the transformation of **1a** into **3a** in methanol under comparable conditions. It seems that the photochemical isomerization of **51** to **55** is so inefficient that the usually dormant [2 + 2] photocycloaddition or 1,3-migration, by which **51** is transformed into **54** by way of **52** or **53**, respectively, becomes operative.[47]

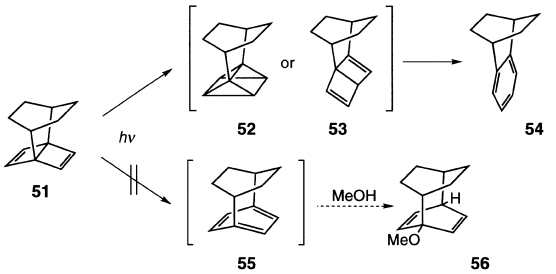

Scheme 14.

Another limiting factor to be considered is the cycloreversion of strained paracyclophanes to the Dewar benzene isomers. As discussed in the preceding section, [4]paracyclophanes are already predicted to lie higher in energy than the corresponding Dewar isomers and **37** indeed thermally reverts fairly rapidly to the Dewar form **43**. The greater the degree of bending of the benzene ring of an [*n*]paracyclophane, the more facile the isomerization to the Dewar benzene form should be. Although **55** would be easily detectable at 77 K, if it were formed from **51**, its thermal cycloreversion to **51** would be much faster than that of **37** to **43**.

2. [1.1]PARACYCLOPHANE SYSTEM

2.1 [1.1]Paracyclophanes The construction of [1.1]-paracyclophane (**59a**), i.e. the connection of two benzene rings at the para positions with two methylene bridges in a cyclic array, apparently requires severe bending of the rings and bonds, and is seemingly almost prohibitive. Despite its fascinating structure, to our knowledge, no report concerning **59** had been published when we embarked on the preparation of **59**. The successful generation of [4]paracyclophanes from the corresponding Dewar benzene precursors, however, suggested that [1.1]paracyclophanes might well be accessible via valence isomerization of the bis(Dewar benzene) isomers **57**. The first step of this isomerization from **57** to **58** is nothing else but the generation of a [4]paracyclophane skeleton, if a stepwise mechanism is assumed, and the second step corresponds to the formation of much less strained, six-carbon-bridged paracyclophane from the respective Dewar benzene precursors (Scheme 15). Thus, the second step should be much easier than the first. This expectation is supported by computational analysis on **57a**–**59a** which reveals, as described later, that the initial step is a slightly endothermic process whereas the second step is highly exothermic. Calculations also indicate that the degree of ring deformation in **59a** will be comparable to that in [5]paracyclophane and much less than that in [4]paracyclophane, implying that **59** might be isolable if electronic interac-

tions between the aromatic rings held in close proximity do not significantly destabilize the system.[48]

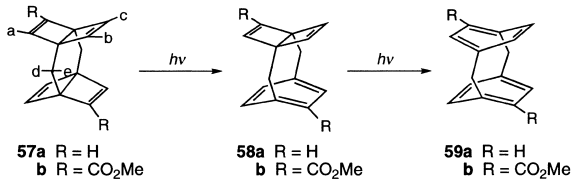

Scheme 15.

(Preparation of Precursors) On the basis of our experience on the preparation of 1,4-bridged Dewar benzenes, we envisioned that the bis(Dewar benzene) precursor **57** might be accessible via a synthetic pathway including two-fold cycloaddition of acetylene or its equivalent to bis(enone) **65** as a key step. Compound **65** was unknown then and, after several unsuccessful attempts, it was eventually synthesized by the acid-catalyzed intramolecular cyclization of unsaturated dicarboxylic acid **64**, which was in turn prepared in four steps from diethyl dihydroterephthalate (**60**). The subsequent transformation of **65** into **57a** and **57b** was carried out in essentially the same manner as described for the preparation of [4.2.2]propellatetraenes **5a,b**, as outlined in Scheme 16. The photocycloaddition of acetylene to **65** proceeded stereoselectively to furnish anti-bis(acetylene) adduct **67a**. The observed stereoselectivity probably results from the preferential bending of the central six-membered ring toward the cyclobutene ring in the monoadduct **66a**, as suggested by force field calculations.

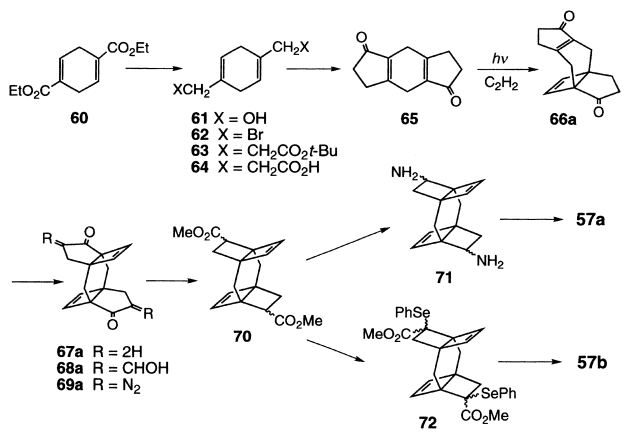

Scheme 16.

(Spectroscopic Detection) The photochemical generation of **59** from **57** was first investigated under matrix isolation at low temperature. Compound **57a** exhibits only an end absorption extending to 260 nm in its electronic absorption spectrum. Irradiation of **57a** in an EPA glass with a low-pressure mercury lamp at 77 K leads to the development of absorption bands at λ_{max} 226, 237, and 290 nm, accompanied by a weak, broad band (λ_{max} 377 nm) in the range of 330–450 nm. These bands are due to **59a** as later assigned. [1.1]Paracyclophane (**59a**) is photochemically labile and the observed absorption rapidly decays upon secondary irradiation of the resulting glass with light of wavelength longer than 335 nm to give rise to a new absorption band at λ_{max} 244 nm, which was later assigned to transannular [4 + 4] adduct **73a** (Scheme 17). The bis(methoxycarbonyl) derivative **57b** displays similar photochemical behavior. Thus, irradiation of **57b** in an EPA glass with light of 254 nm at 77 K gives rise to **59b**, which exhibits absorption bands at λ_{max} 256 and 348 nm, accompanied by a weak, broad band (λ_{max} 405 nm) extending to 480 nm. The latter is efficiently transformed into **73b** upon secondary irradiation. Broad, relatively weak bands in the long wavelength region in the absorption spectra of **59a** and **59b** are a characteristic feature common to [1.1]paracyclophanes. Those bands, probably of forbidden transitions, suggest significant electronic interactions between the two bent benzene moieties of [1.1]paracyclophane. The photochemical transannular addition within **59** to give **73**, to our knowledge, represents the first direct formation of a benzene *p,p′*-dimer and is certainly a consequence of the face-to-face arrangement of the bent benzene rings in close proximity.[49]

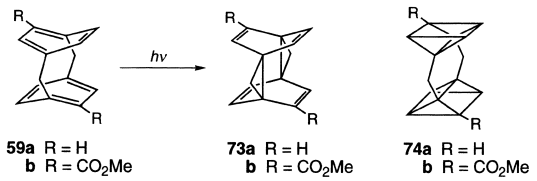

Scheme 17.

The thermal stabilities of **59a** and **59b** are much superior to those of [4]paracyclophanes and their UV-visible absorption spectra remain unchanged for several hours if their solutions are kept below −20 °C. At higher temperatures, however, the absorptions begin to decay and almost completely disappear within 4 hours at room temperature, practically preventing isolation of the compounds. The decomposition products are resinous materials, probably resulting from polymerization at the most strained bridgehead carbon atoms.

Although [1.1]paracyclophanes **59a,b**, to our disappointment, lack sufficient stability to allow their isolation, their ^{1}H NMR spectra have been recorded. The Dewar benzene precursor **57b** exhibits a simple ^{1}H NMR spectrum consistent with its C_i symmetric structure at least on the ^{1}H NMR time scale. Irradiation of **57b** in THF-d_8 with a low-pressure mercury lamp at −70 °C leads to the formation of two species in a ratio of ca. 1 : 2 after 10% conversion. Both the species also retain the C_i symmetry and the minor product is quantitatively converted into the major one upon secondary irradiation of the mixture with filtered light (> 390 nm). On the basis of these observations and their spectral characteristics, structures **59b** and **73b** were assigned to the former and the latter, respectively. The observed changes in chemical shift and in coupling constant are fully consistent with the successive transformation of **57b** into **59b**, and **59b** into **73b** (Table 8). Neither the less symmetrical products resulting from the rearrangement in only one of the Dewar benzenes, i.e. **58b**, nor the diprismane derivative **74b** is detected in the photolysate. The transannular adduct **73b** is also photochemically susceptible and extended irradia-

Table 8. ^{1}H NMR Parameters for **57b**, **59b**, and **73b**[a), 9]

Compound	$H_a(\delta)$	J_{ab}/Hz	H_b,$H_c(\delta)$	J_{bc}/Hz	H_d,$H_e(\delta)$	J_{de}/Hz
57b	7.19	< 1	6.45, 6.56	2.4	2.38, 2.50	14.6
59b	7.60	2.5	6.95, 7.14	8.8	4.44[b)]	11.7
73b	7.12	< 1	6.03, 6.13	6.4	1.95, 2.45	6.6

a) In THF-d_8 at −60 °C. The signals of OCH_3 were observed at δ 3.65, 3.94, and 3.61 for **57b**, **59b**, and **73b**, respectively. b) The signal of the other proton could not be identified, probably due to its overlap with one of the much stronger signals due to the methoxy group of **57b** at δ 3.65, the solvent at δ 3.58, and water at δ 3.30.

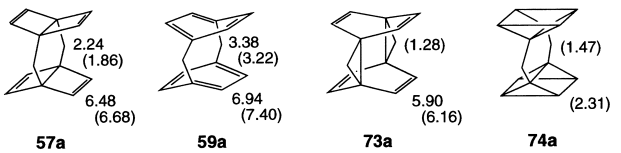

Fig. 7. Experimental and calculated (in parentheses) proton chemical shifts for **57a**, **59a**, **73a**, and **74a**.

tion of the mixture does not bring about an appreciable increase in its amount, but induces decomposition of **57b** and the products.

Irradiation of **57a** in THF-d_8 with a low-pressure mercury lamp at −80 °C leads to the development of singlet signals assignable to **59a** and **73a**. The observed spectra were, however, extremely simple and of low relative intensities, and could well happen to be due to unknown side products. Therefore, recourse to theoretical calculations was made to confirm the structural assignments. The experimental and computed (GIAO/6-31G*//6-31G*) proton chemical shifts for **57a**, **59a**, and **73a**, summarized in Fig. 7, are in reasonable agreement with each other, supporting the above structural assignment. The diprismane product **74a** of the same symmetry is apparently incompatible with either of the observed spectra. Again the formation of mono-aromatized **58a** was not detected.

It is of interest to compare the ^{1}H NMR spectra of **59a** and **59b** with those of the corresponding [2.2]paracyclophane homologues. The aromatic ring protons of [2.2]paracyclophane resonate at δ 6.47 and the [2.2]paracyclophane counterparts to the H_A–H_C of **59b** resonate at δ 7.17 (J = 1.8 Hz), 6.68 (dd, J = 7.7 and 1.8 Hz), and 6.51 (d, J = 7.7 Hz), respectively.[50] Thus the chemical shifts of aromatic protons in the [1.1]paracyclophanes are rather normal while those in the [2.2]paracyclophanes resonate 0.4–0.5 ppm upfield. The upfield shifts of aromatic proton signals in [2.2]paracyclophanes suggest that they are exposed to a shielding effect by the opposing aromatic ring. The closer juxtaposition of the aromatic rings, in addition to the more pronounced inward bending of the aromatic C–H bonds, in [1.1]paracyclophane than in [2.2]paracyclophane, may place the aromatic protons of the former near the boundary plane between the shielding and deshielding fields due to the ring current in the facing benzene ring.

(Computational Analysis) The geometrical as well as electronic structures of [1.1]paracyclophane, its strain energy and thermodynamic stability relative to related compounds, and the degree of aromaticity retained in it are of special interest. To gain insights into these points, theoretical analyses were carried out by ab initio and DFT quantum mechanical methods.

The geometrical optimizations of **59a** and **73a** were undertaken at the Hartree–Fock (RHF-SCF), second-order perturbation (MP2), and density functional B3LYP levels employing 6-31G* basis set. The structures of the related compounds, **57a** and **58a**, were also optimized at the RHF/6-31G* level and with semiempirical MNDO Hamiltonian. An initial exploration of the potential energy surface of **59a** with the 3-21G basis set furnished a single energy minimum corresponding to the D_{2h} symmetric **59a**. The optimizations with the 6-31G* basis set were accordingly performed within the constraint of D_{2h} symmetry. The optimized geometrical parameters for **59a** are summarized in Tables 9 and 10.[9b]

The differences between the optimized geometries of **59a** are generally small, Δ(bond length) ≤ 0.014 Å and Δ(bond angle) ≤ 0.7°. The transannular distance R_1 is in a range of 2.36–2.40 Å, almost 1.0 Å less than the sum of the van der Waals radii, suggesting strong electronic interactions between the π bonds of the opposing aromatic rings. These calculated parameters are in good agreement with the experimental values for the heavily substituted derivative described later. The extent of bond alternation in the aromatic rings is small, indicating the retention of cyclic delocalization of electrons in the bent benzene rings. The calculated bending angles α and β slightly deviate from the experimental values provided in the following section, but the calculated and experimental total deformation angles ($\alpha + \beta$) agree excellently with each other. The angle ($\alpha + \beta$) in **59a** is much smaller than that calculated for [4]paracyclophane and even slightly smaller than that for [5]paracyclophane. In accord with the calculation results, **59a** is much superior to the former and is comparable to the latter in kinetic stability. Thus, it appears that the reactivity of **59a** is primarily determined by the extent of bending of the aromatic rings and **59a** is neither particularly stabilized nor particularly destabilized by the close stacking of the benzene rings.

Relative energies callculated for **59a** and relevant related compounds are collected in Table 11. Inspection of the Table reveals that **59a** is predicted to be the most stable of the isomers and more stable than **73a**, irrespective of the computation methods and theoretical levels employed. The calculations also indicate that the isomerization of **57a** to **58a** is endothermic whereas that of **58a** to **59a** is strongly exothermic, suggesting that the latter process is significantly more facile than the former. Accordingly, it is not unreasonable that **58a** and **58b** are not detected in the photolysates of **57a** and **57b**, respectively, though a stepwise mechanism is likely in operation. Although **59a** is the most stable of the calculated isomers, it is still a highly strained molecule. For the evaluation of strain

Table 9. Calculated Distortion Angles and Nonbonding Interatomic Distances for [1.1]- and [2.2]Paracyclophanes

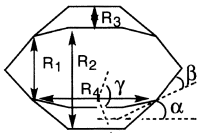

Method	α/deg	β/deg	$(\alpha+\beta)$/deg	γ/deg	R_1/Å	R_2/Å	R_3/Å	R_4/Å
			[1.1]Paracyclophane					
RHF/6-31G*	23.7	26.3	50.0	28.6	2.383	2.982	2.351	2.761
B3LYP/6-31G*	23.3	27.0	50.3	28.3	2.396	2.995	2.371	2.787
MP2/6-31G*	22.5	27.4	49.9	27.2	2.363	2.938	2.378	2.792
			[2.2]Paracyclophane[51]					
experimental	12.6	11.2	23.8		2.778	3.093		

Table 10. Calculated Bond Angles and Bond Lengths for [1.1]Paracyclophane

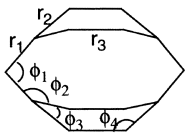

Method	r_1/Å	r_2/Å	r_3/Å	ϕ_1/deg	ϕ_2/deg	ϕ_3/deg	ϕ_4/deg
RHF/6-31G*	1.557	1.393	1.390	99.8	118.3	115.1	119.5
B3LYP/6-31G*	1.558	1.406	1.400	100.5	118.6	115.0	118.6
MP2/6-31G*	1.545	1.407	1.401	99.8	118.3	115.3	119.6

Table 11. Calculated Energies of **57a**, **58a**, and **73a** Relative to **59a** (in kcal mol^{-1})

Method	**57a**	**58a**	**59a**	**73a**
MNDO	41.1	49.6	0	9.7
RHF/6-31G*	51.5	62.3	0	8.7
MP2/6-31G*			0	20.0
B3LYP/6-31G*	70.7		0	25.6

energy in **59a**, 9,10-dihydroanthracene, which also possesses two benzene rings bridged by two methylenes as **59a** and yet is strain-free, serves as an ideal reference compound. The total strain energy of **59a** thus evaluated is 128.1, 93.6, and 106.5 kcal mol^{-1} at the RHF/6-31G*, MP2/6-31G*, and B3LYP/6-31G* levels, respectively, and is in good agreement with the values evaluated using the homodesmotic reaction of eq 2, 127.8 kcal mol^{-1} at the RHF/6-31G* level and 90.8 kcal/mol at the MP2/6-31G* level.

$$C_{14}H_{12}\ (\mathbf{59a}) + 4\ C_2H_6 \rightarrow 2\ p\text{-}C_6H_4Me_2 + 2\ C_3H_8 \quad (2)$$

The close face-to-face arrangement of the two bent aromatic rings in **59a** suggests strong electronic interactions between them. The RHF/6-31G* calculations confirm that the HOMO and LUMO of **59a** are significantly raised and lowered in energy, respectively, as compared to those of *p*-xylene as the result of bending of the benzene rings and of their mutual electronic coupling. Figure 8 depicts a qualitative derivation of the high energy occupied and low energy unoccupied molecular orbitals of **59a** from those of planar *p*-xylene. The distortion of

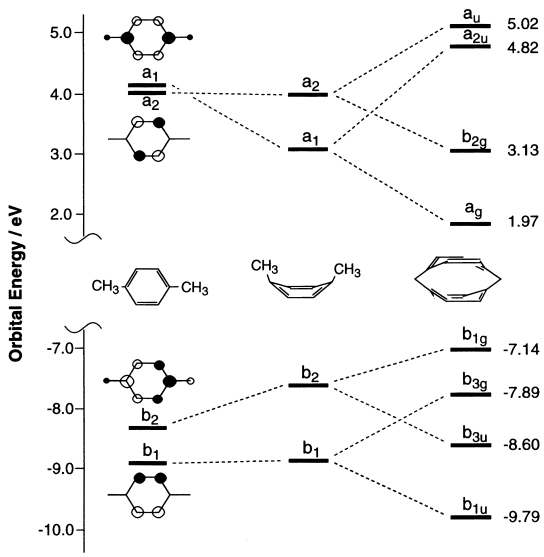

Fig. 8. Derivation of the high energy occupied and low energy unoccupied MOs of [1.1]paracyclophane from those of planar C_{2v}-*p*-xylene (SCF/6-31G*).

C_{2v}-*p*-xylene to the geometry present in **59a** leads to the destabilization of $b_2(\pi)$ and the stabilization of $a_1(\pi^*)$ MO, while leaving the a_2 and b_1 MOs virtually unperturbed. The through-space and -bond coupling of the resulting b_2 orbitals in **59a** yields b_{1g} and b_{3u} MOs and that of the a_1 MOs leads to MOs of a_g and a_{2u} symmetries. The a_2 and b_1 MOs mutually interact respectively, predominantly through space, to yield the b_{3g}/b_{1u} and a_u/b_{2g} MOs of **59a** (Fig. 9). The reduced HOMO–LUMO

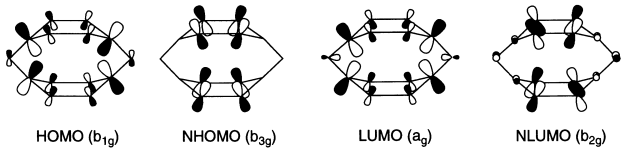

Fig. 9. Schematic representations of the HOMO, NHOMO, LUMO, and NLUMO of [1.1]paracyclophane (N denotes next).

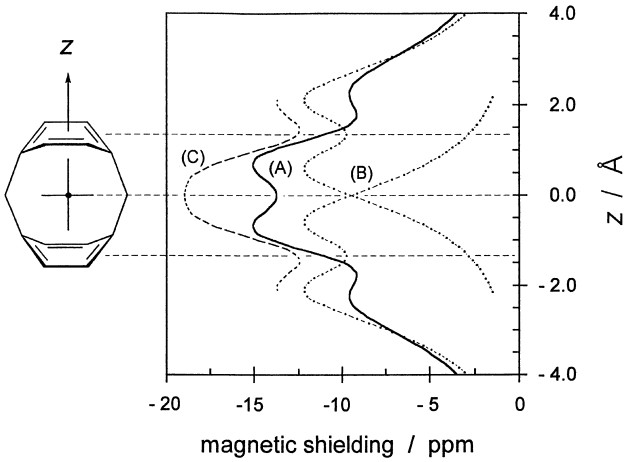

Fig. 10. Variation of magnetic shielding effect (in ppm) in **59a** along the *z* coordinate and comparison with the effect due to two molecules of benzene (GIAO/6-31+G*//B3LYP/6-31G*): (A) for **59a**, (B) for two benzene molecules at the same mean distances with the aromatic rings of **59a** from the center of gravity of the latter, and (C) sum of the effects due to the two molecules of benzene. Negative value denotes diamagnetic shielding.

energy gap in **59a** (8.83 eV) as compared to that in *p*-xylene (12.33 eV) manifests itself in the UV-visible absorption spectrum extending to 450 nm.

It is of particular interest to investigate how the diamagnetic property of [1.1]paracyclophane is affected by those geometrical and electronic perturbations. Figure 10 illustrates the plot of NICS value for **59a** against the distance from the center of molecule along the *z* coordinate computed at the GIAO/6-31+G*//B3LYP/6-31G* level, together with those for planar benzene rings placed at the same mean distances as in **59a** and their sum. The partially reduced diamagnetic shielding in **59a** as compared to the sum of the effects due to the two planar benzene molecules suggests that **59a** sustains slightly diminished diamagnetic ring current and hence loses some aromaticity owing to the geometrical constraints imposed on its structure.

2.2 Kinetic Stabilization of [1.1]Paracyclophane The fact that the stabilities of **59a** and **59b** were insufficient to allow isolation prompted us to search for a way to kinetically stabilize the [1.1]paracyclophane skeleton without disturbing its essential properties. The instability of [1.1]paracyclophane seems to arise from susceptibility of the bridgehead carbon atoms toward addition of various reagents, as is the case with [4]paracyclophane and its derivatives. Accordingly, we next investigated the feasibility of stabilizing the skeleton of [1.1]paracyclophane kinetically by introducing substituents that sterically shield all four bridgehead sites.

Substituents conventionally used for such a purpose are sterically demanding, inert ones whose bulkiness remains largely unaffected by conformational changes, like *t*-butyl. Synthetic difficulty accompanying the introduction of such substituents into the bis(Dewar benzene) precursor **57**, however, seemed insurmountable. Fortunately, examination of molecular models suggested that kinetic stabilization of the [1.1]paracyclophane system may be achieved through **59c**, for which the appropriate precursor **57c** should also be accessible (Scheme 18). The substituents in **59c**, trimethylsilylmethyl and dimethylcarbamoyl, are conformationally flexible and the effective bulkiness is very much dependent on their adopted conformations, yet they are expected to shield the bridgehead carbon atoms of **59c** from access by attacking reagents in the most preferred conformation. For the construction of 1,4-bridged Dewar benzene skeletons, we have so far resorted to the photo-Wolff ring contraction of diazocyclopentanone derivatives to the corresponding cyclobutanecarboxylic acid derivatives. While the dimethylcarbamoyl group on the aromatic ring of [1.1]paracyclophane seemed to exert a substantial stabilizing effect by placing one of the methyl groups over the proximate bridgehead carbon atom, the corresponding alkoxycarbonyl substituent appeared not to contribute appreciably to the steric protection of the skeleton. These expectations were experimentally verified, as described later.

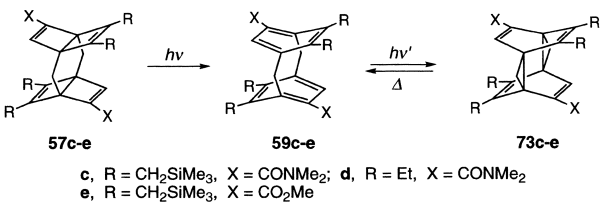

Scheme 18.

(Preparation of the Bis(Dewar benzene) Precursors) The preparation of the substituted bis(Dewar benzene) precursors **57c–e** was carried out in essentially the same manner as described for **57a,b**, except for a few critical modifications (Schemes 19 and 20). Thus, the two-fold [2 + 2] photocycloaddition of 1,4-bis(trimethylsilyl)-2-butyne (**75**)[38] to **65** followed by the diazotization and photo-Wolff ring contraction in MeOH furnished **76**, while the photo-Wolff rearrangement in an aprotic solvent provided diketene **78**, from which diamide **82** was prepared by the addition of $LiNMe_2$ followed by hydrolysis. However, ester **76** and amide **82** are already so sterically crowded that attempts to α-phenylselenenylate them met with difficulty. Thus, neither treatment of **76** with LDA/PhSeBr nor attempts to react PhSeBr with the enolate ion which was generated from **78** and MeONa[52] provided the desired product. For the selenenylation of sterically hindered esters, their treatment with KH in the presence of $(PhSe)_2$ has been recommended.[53] Application of this method to **76** followed by the usual oxidation-elimination reaction resulted in the formation of **77** in a modest yield. Through the repetition of the

same reaction sequence, **77** was finally converted into **57e**.

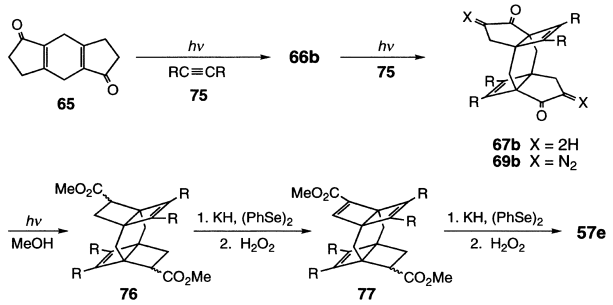

Scheme 19. (R = CH_2SiMe_3).

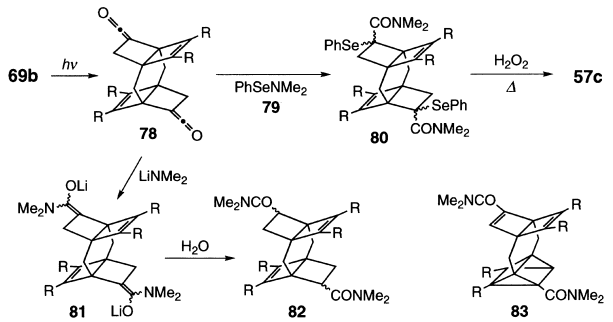

Scheme 20. (R = CH_2SiMe_3).

The selenenylation of **82** was all the more difficult and the above methods proved useless. Selenenamide **79** adds to the carbon–carbon double bond of conjugated enone by way of the initial formation of zwitterion **84** followed by intramolecular migration of the phenylselenyl group (Scheme 21).[54] The central carbon atoms of the ketene moieties of **78** are apparently less sterically encumbered than the carbon atoms adjacent to the amide groups of **82**. If **79** is able to add to ketene to generate zwitterionic intermediate **85**, α-selenenylated amide **86** may well be produced through the subsequent migration of the phenylselenyl group. This hypothetical reaction worked excellently and treatment of **78** with **79** furnished **80**, from which **57c** was obtained following the usual oxidation-elimination protocol. The less sterically crowded amide **57d** was also prepared in the same manner from the twofold adduct of 3-hexyne to **65**.

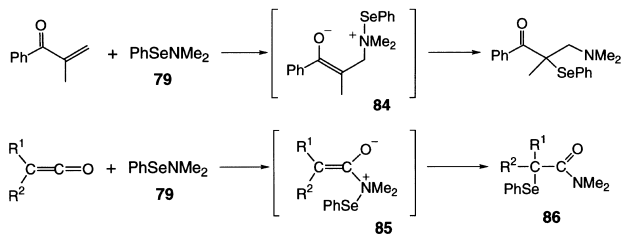

Scheme 21.

(Isolation of a Kinetically Stabilized [1.1]Paracyclophane) Amide **57c** exhibits a featureless electronic absorption spectrum extending to 350 nm. Irradiation of **57c** in degassed *n*-decane with a low-pressure mercury lamp at −20 °C leads to the formation of **59c** (λ_{max} 321, 377, and 464 nm), isomer **73c** resulting from a secondary transannular [4 + 4] addition within **59c**, and a product to which structure **83** is tentatively assigned. The intensity of the UV-visible absorption bands due to **59c** remains unchanged for 3 h at 50 °C and decreases only by 8% after the solution is heated for 2 h at 100 °C, demonstrating the greatly improved stability of **59c** as compared to that of **57a** or **57b**. Compounds **57d** and **57e** also underwent successive phototransformation into **59d** and **59e**, and then into **73d** and **73e**, respectively. The kinetic stability of **59d** is significantly inferior to **59e**, which is in turn substantially less stable than **59c**, as summarized in Scheme 22. This order of kinetic stabilities is in accord with predictions based on molecular modeling.

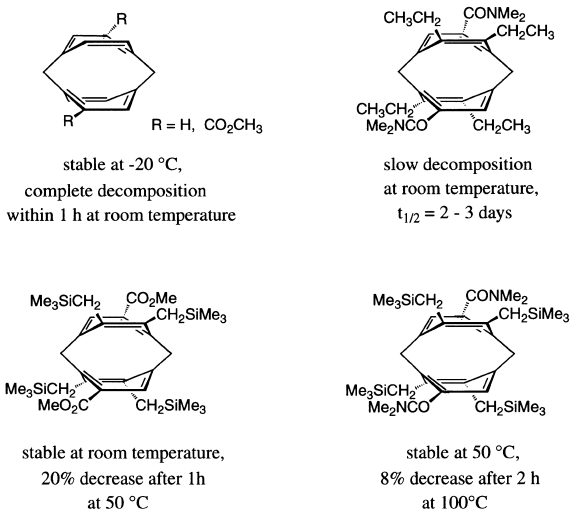

Scheme 22.

When a solution of **59c** was irradiated to furnish **73c** and then allowed to stand in the dark at room temperature, the characteristic UV-visible absorption due to **59c** was slowly regenerated. This observation demonstrates the ability of **73c** to thermally revert to **59c** at ambient or higher temperature! The corresponding cycloreversion is also observed for **73d** and **73e**. This reactivity of **73** proved to be quite advantageous to the preparation and purification of air-sensitive **59** because the latter is difficult to prepare directly from **57** in pure form in reasonable yield. The photochemical isomerization of **57** tends to produce mainly **73** rather than the primary product **59**, except at very low conversion, because **59** is very susceptible to photochemical transformation into **73** and, moreover, its high absorptivity extends to a wavelength much longer than that of the precursor **57**. Air-stable **73c** is readily isolated from the mixture as colorless crystals, and it can be quantitatively converted into **59c** by mildly heating its solution in a deaerated solvent such as benzene or hexane. Thus, the fairly air-sensitive **59c** is now readily prepared in pure form. When a solution of **73c** in degassed benzene was heated at 45 °C for 15 h and then cooled to 5 °C, the resulting **59c** separated from solution in the form of orange-red crystals.

Figure 11 illustrates the development of electronic absorption due to **59c** upon heating a solution of **73c** in hexane at 40 °C. The thermal isomerization follows first-order kinetics and

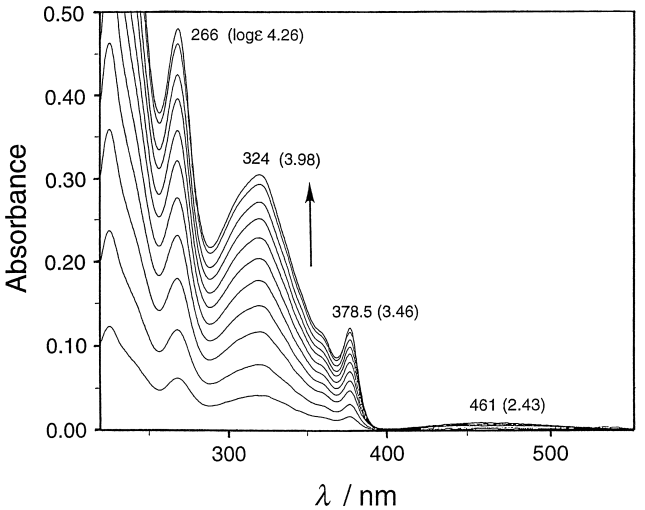

Fig. 11. Development of UV–vis absorption due to **59c** recorded at 15 min intervals upon heating a solution of **73c** in hexane at 40 °C.

activation parameters for the process are: $\Delta G^{\ddagger} = 24.4$ kcal mol^{-1} at 40 °C, $\Delta H^{\ddagger} = 21.1 \pm 0.8$ kcal mol^{-1}, and $\Delta S^{\ddagger} = -10.5 \pm 2.6$ cal K^{-1} mol^{-1}. The half-life of **73c** at 40 °C is 191 ± 2 min in hexane. Scheme 23 lists activation parameters for the cycloreversion of related benzene *p*,*p*′-dimers **87–89**, for comparison purposes. The values for **73c** are rather surprisingly comparable to those for **87** and **88**,[55,56] despite tremendous differences in the heats of reaction.[57] The effect of the lesser exothermicity of the process on the activation energy for **73c** may be counterbalanced by the lesser strength of cleaving (cyclopropane) bonds.

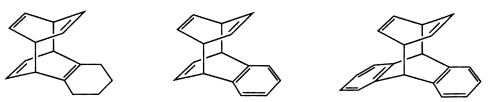

	87	**88**	**89**
$\Delta G^{\ddagger}$ (kcal/mol)	22.0 (0 °C)	23.2 (30 °C)	27.2 (80 °C)
$\Delta H^{\ddagger}$ (kcal/mol)	22.4 ± 1.2	22.8 ± 0.4	33.0 ± 0.9
$\Delta S^{\ddagger}$ (cal/K•mol)	0.9 ± 3.9	-1.4 ± 1.3	16.4 ± 2.4

Scheme 23.

(X-ray Crystallographic Analysis) The molecular structures of **59c** and **73c** are given in Figs. 12 and 13, respectively. Both **59c** and **73c** have C_i symmetry in the crystalline state and their polycyclic cores are slightly distorted from ideal D_{2h} symmetry. The transannular interatomic distance between the opposing bridgehead carbon atoms C(1)–C(4′) of **59c** is 2.376(5) Å, less than the sum of the van der Waals radii (3.5–3.6 Å)[58] by more than 1.0 Å, and the corresponding distances between nonbridgehead aromatic carbon atoms C(2)–C(5′) and C(3)–C(6′) are 3.025(5) and 2.996(5) Å, respectively. The dihedral angle α between the mean plane of the four nonbridgehead carbon atoms and the plane of the adjoining flap is 25.6° on the side bearing the amide group and 24.3° on the other. The extent of out-of-plane bending of the bridging bonds β is 26.8° on the side nearer to the amide group and 22.9° on the far side.[59] Thus, the averaged total bending angle ($\alpha + \beta$) is

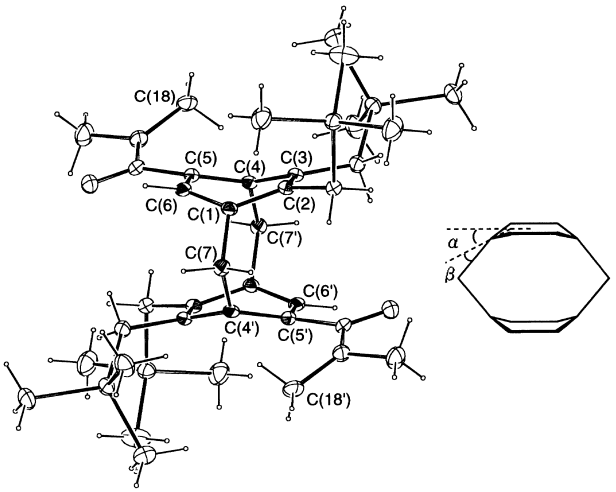

Fig. 12. Crystal structure of **59c**. Selected bond lengths (Å), nonbonding interatomic distances (Å), and angles (°) are: C(1)–C(2), 1.443(6); C(2)–C(3), 1.396(6); C(3)–C(4), 1.422(6); C(4)–C(5), 1.421(6); C(5)–C(6), 1.400(6); C(1)–C(6), 1.386(6); C(1)–C(7), 1.551(6); C(4)–C(7′), 1.560(6); C(1)···C(4′), 2.376(5); C(2)···C(5′), 3.025(5); C(3)···C(6′), 2.996(5); C(1)···C(4), 2.760(5); C(1)–C(2)–C(3), 117.6(4); C(2)–C(3)–C(4), 119.3(4); C(3)–C(4)–C(5), 116.5(4); C(4)–C(5)–C(6), 116.4(4); C(5)–C(6)–C(1); 121.6(4); C(2)–C(1)–C(6), 115.4(4); C(2)–C(1)–C(7), 120.9(4); C(6)–C(1)–C(7), 118.2(4); C(1)–C(7)–C(4′), 99.6(3).

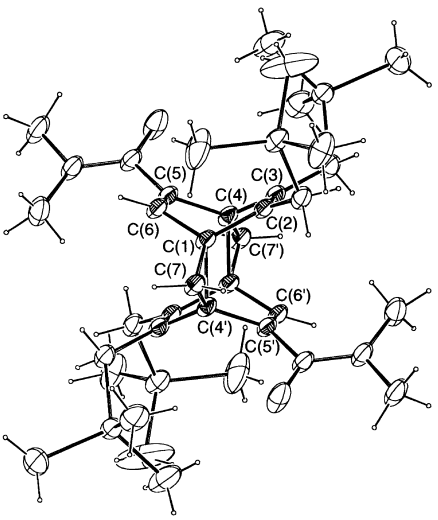

Fig. 13. Crystal structure of **73c**. Selected bond lengths (Å), nonbonding interatomic distances (Å), and angles (°) are: C(1)–C(2), 1.508(2); C(2)–C(3), 1.350(2); C(3)–C(4), 1.516(2); C(4)–C(5), 1.505(2); C(5)–C(6), 1.345(2); C(1)–C(6), 1.494(2); C(1)–C(4′), 1.601(2); C(1)–C(7), 1.499(2); C(4)–C(7′), 1.494(2); C(2)···C(5′), 2.789(2); C(3)···C(6′), 2.808(2); C(1)···C(4), 2.519(2); C(1)–C(2)–C(3), 112.8(2); C(2)–C(3)–C(4), 112.7(2); C(3)–C(4)–C(5), 112.5(1); C(4)–C(5)–C(6), 112.3(2); C(5)–C(6)–C(1), 113.8(2); C(2)–C(1)–C(6), 112.2(1); C(1)–C(4′)–C(7), 57.8(1); C(1)–C(7)–C(4′), 64.7(1); C(4′)–C(1)–C(7), 57.5(1).

49.8°, which is the largest value ever observed for a paracyclophane[60] and only slightly less than that calculated for

[5]paracyclophane. The bonds of methylene bridges are lengthened from normal 1.50–1.52 Å to 1.55–1.56 Å, probably due to the steric repulsion between the aromatic rings, while the bond angle, C(1)–C(7)–C(4′), is narrowed from 112.5° in diphenylmethane[61] to 99.6° to accommodate planarity-preferring benzene rings in the [1.1]paracyclophane structure.

In good agreement with the results of molecular modeling, the nearly planar amide group adopts *s*-trans conformation, with respect to the adjacent bridgehead carbon atom, placing one of the methyl groups (C(18) and C(18′)) above the bridgehead site. Preferential adoption of a similar conformation in solution is supported by the NOE experiments. The inferior kinetic stability of ester **59e** as compared to amide **59c** is most probably due to the lack of a corresponding methyl group protruding above the neighboring bridgehead site, as presumed on the basis of molecular modeling. The trimethylsilyl groups preferentially occupy the space near the proximate bridgehead carbon atom to sterically hinder the access of other reagents to the latter, thereby minimizing repulsive steric interactions: mutual, transannular, and with the methylene bridges. Thus, the bridgehead carbon atoms of **59c** are effectively protected by the aromatic substituents: this is certainly the reason for its remarkable stability.

The most prominent feature in the structure of **73c** is the unusual lengthening of the inner cyclopropane bonds to 1.601(2) Å. They are longer by 0.10–0.11 Å than the peripheral cyclopropane bonds, while the latter appear to be slightly shortened from a bond length of 1.51 Å for cyclopropane. Compound **73c** possesses the structure of benzene *p*,*p*′-dimer bridged by methylenes. Similar lengthening of bond has been observed for related dibenzene structures[62] and, to explain the anomalous bond lengthening, π–σ–π through-bond coupling[63] has used to be invoked. Siegel and co-workers recently questioned this explanation and have asserted that steric/electrostatic repulsion is the dominant cause of bond elongation.[64] Nonbonding interatomic distances between the proximate unsaturated carbon atoms C(2)···C(5′) and C(3)···C(6′) are only 2.789 and 2.808 Å, respectively, and thus significantly shorter than the sum of the van der Waals radii. It is interesting to note in this respect that the length of the inner cyclopropane bond of **73c** is reproduced satisfactorily by the theoretical calculations for the parent **73a** at both the B3LYP/6-31G* (1.607 Å) and MP2/6-31G* (1.597 Å) levels, but only poorly at the RHF/6-31G* level (1.564 Å) and by the semiempirical AM1 (1.563 Å) and PM3 (1.548 Å) methods.

Sincere thanks are due to our co-workers for their dedication and enthusiasm. Their names are cited in the literature references. T.T. also thanks the Computer Center of the Institute for Molecular Science for the use of computers. Continued support of our work on strained paracyclophanes by the Ministry of Education, Science, Sports and Culture is gratefully acknowledged.

References

1 a) F.Bickelhaupt and W. H. de Wolf, *Recl. Trav. Chim. Pays-Bas*, **107**, 459 (1988); b) F. Bickelhaupt and W. H. de Wolf, in "Advances in Strain in Organic Chemistry," ed by B. Halton, JAI Press, Greenwich, Ct. (1993), Vol. 3, pp. 185–227. c) Y. Tobe, in "Topics in Current Chemistry," ed by E. Weber, Springer, Berlin (1994), Vol. 172, pp. 1–40. d) V. V. Kane, W. H. de Wolf, and F. Bickelhaupt, *Tetrahedron*, **50**, 4575 (1994). e) A. de Meijere and B. König, *Synlett*., **1997**, 1221.

2 T. Tsuji, in "Advances in Strained and Interesting Organic Molecules," ed by B. Halton, JAI Press, Stamford, Ct. (1999), Vol. 7, pp. 103–152.

3 a) N. L. Allinger and T. J. Walter, *J. Am. Chem. Soc*., **94**, 9267 (1972). b) G. M. Newton, T. J. Walter, and N. L. Allinger, *J. Am. Chem. Soc*., **95**, 5652 (1973). c) A. D. Wolf, V. V. Kane, R. H. Levin, and M. Jones, Jr., *J. Am. Chem. Soc*., **95**, 680 (1973). d) J. W. van Straten, W. H. de Wolf, and F. Bickelhaupt, *Recl. Trav. Chim. Pays-Bas*, **96**, 88 (1977). e) L. W. Jenneskens, W. H. de Wolf, and F. Bickelhaupt, *Tetrahedron*, **42**, 1571 (1986). f) P. G. Gassman, T. F. Bailey, and R. C. Hoye, *J. Org. Chem*., **45**, 2923 (1980). g) J. Hünger, C. Wolff, W. Tochtermann, E. M. Peters, K. Peters, and H. G. von Schnering, *Chem. Ber*., **119**, 2698 (1986).

4 a) V. V. Kane, A. D. Wolf, and M. Jones, Jr., *J. Am. Chem. Soc*., **96**, 2643 (1974). b) S. L. Kammula, L. D. Iroff, M. Jones, Jr., J. W. van Straten, W. H. de Wolff, and F. Bickelhaupt, *J. Am. Chem. Soc*., **99**, 5815 (1977). c) J. Liebe, C. Wolff, and W. Tochtermann, *Tetrahedron Lett*., **23**, 171 (1982). d) Y. Tobe, K. Kakiuchi, Y. Odaira, T. Hosaki, Y. Kai, and N. Kasai, *J. Am. Chem. Soc*., **105**, 1376 (1983). e) J. Liebe, C. Wolff, C. Krieger, J. Weiss, and W. Tochtermann, *Chem. Ber*., **118**, 4144 (1985). f) J. L. Jessen, C. Wolff, and W. Tochtermann, *Chem. Ber*., **119**, 297 (1986). g) Y. Tobe, K. Ueda, K. Kakiuchi, Y. Odaira, Y. Kai, and N. Kasai, *Tetrahedron*, **42**, 1851 (1986). h) Y. Tobe, K. Ueda, T. Kameda, K. Kakiuchi, Y. Odaira, and N. Kasai, *J. Am. Chem. Soc*., **109**, 1136 (1987). i) R. Gleiter and B. Treptow, *Angew. Chem., Int. Ed. Engl*., **29**, 1429 (1990).

5 a) L. W. Jenneskens, F. J. J. de Kanter, P. A. Kraakman, L. A. M. Turkenburg, W. E. Koolhaas, W. H. de Wolff, F. Bickelhaupt, Y. Tobe, K. Kakiuchi, and Y. Odaira, *J. Am. Chem. Soc*., **107**, 3716 (1985). b) Y. Tobe, T. Kaneda, K. Kakiuchi, and Y. Odaira, *Chem. Lett*., **1985**, 1301. c) G. B. M. Kostermans, W. H. de Wolff, and F. Bickelhaupt, *Tetrahedron*, **43**, 2955 (1987). d) D. S. Van Es, F. J. J. de Kanter, W. H. de Wolf, and F. Bickelhaupt, *Angew. Chem., Int. Ed. Engl*., **34**, 2553 (1995).

6 G. B. M. Kostermans, M. Bobeldijk, W. H. De Wolf, and F. Bickelhaupt, *J. Am. Chem. Soc*., **109**, 2471 (1987).

7 T. Tsuji and S. Nishida, *J. Chem. Soc., Chem. Commun*., **1987**, 1189. *J. Am. Chem. Soc*., **110**, 2157 (1988).

8 a) C. J. Brown and A. C. Farthing, *Nature*, **164**, 915 (1949). b) C. J. Brown, *J. Chem. Soc*., **1953**, 3265.

9 a) T. Tsuji, M. Ohkita, and S. Nishida, *J. Am. Chem. Soc*., **115**, 5284 (1993). b) T. Tsuji, M. Ohkita, T. Konno, and S. Nishida, *J. Am. Chem. Soc*., **119**, 8425 (1997).

10 H. Kawai, T. Suzuki, M. Ohkita, and T. Tsuji, *Angew. Chem., Int. Ed. Engl*., **37**, 817 (1998); *Chem. Eur. J*., **6**, 4177 (2000).

11 G. Kaupp, *Angew. Chem., Int. Ed. Engl*., **15**, 442 (1976).

12 L. W. Jenneskens, J. N. Louwen, W. H. de Wolf, and F. Bickelhaupt, *J. Phys. Org. Chem*., **3**, 295 (1990).

13 S. Grimme, *J. Am. Chem. Soc*., **114**, 10542 (1992).

14 B. Ma, H. M. Sulzbach, R. B. Remington, and H. F. Schaefer III, *J. Am. Chem. Soc*., **117**, 8392 (1995).

15 a) P. Lecktken, R. Brelow, A. H. Schmidt, and N. J. Turro, *J. Am. Chem. Soc*., **95**, 3025 (1973). b) N. J. Turro and V. Ramamurthy, in "Rearrangements in Ground and Excited States," ed by P. de Mayo, Academic Press, New York (1980), Vol. 3, pp.

1–23.

16 M. von Arnim and S. D. Peyerimhoff, *Theor. Chim. Acta*, **85**, 43 (1993).

17 M. Okuyama, M. Ohkita, and T. Tsuji, *J. Chem. Soc., Chem. Commun.*, **1997**, 1277.

18 F. Bockisch, J. C. Rayez, D. Liotard, and B. Duguay, *J. Mol. Struct.*, **284**, 75 (1993).

19 J. R. Wiseman and J. J. Vanderbilt, *J. Am. Chem. Soc.*, **100**, 7730 (1978).

20 a) K. B. Wiberg, M. G. Matturro, P. J. Okarma, and M. E. Jason, *J. Am. Chem. Soc.*, **106**, 2194 (1984). b) K. B. Wiberg, R. D. Adams, P. J. Okarma, M. G. Matturro, and B. Segmuller, *J. Am. Chem. Soc.*, **106**, 2200 (1984).

21 R. L. Viavattene, F. D. Greene, L. D. Cheung, R. Majeste, and L. M. Trefonas, *J. Am. Chem. Soc.*, **96**, 4342 (1974).

22 a) T. Tsuji and S. Nishida, *J. Am. Chem. Soc.*, **111**, 368 (1989). b) T. Tsuji, S. Nishida, M. Okuyama, and E. Osawa, *J. Am. Chem. Soc.*, **117**, 9804 (1995).

23 a) T. Tsuji, Z. Komiya, and S. Nishida, *Tetrahedron Lett.*, **21**, 3583 (1980). b) T. Tsuji and S. Nishida, *Tetrahedron Lett.*, **24**, 3361 (1983).

24 H. J. Reich and S. Wollowitz, *Org. React.*, **44**, 1 (1993).

25 a) T. Shioiri, K. Ninomiya, and S. Yamada, *J. Am. Chem. Soc.*, **94**, 6203 (1972). b) K. Ninomiya, T. Shioiri, and S. Yamada, *Tetrahedron*, **30**, 2151 (1974).

26 R. Gleiter, G. Krennrich, P. Bischof, T. Tsuji, and S. Nishida, *Helv. Chim. Acta*, **69**, 962 (1986).

27 a) A. Greenberg and J. F. Liebman, "Strained Organic Molecules," Academic Press, New York (1978). b) K. J. Shea, *Tetrahedron*, **36**, 1683 (1980). c) G. Szeimies, in "Reactive Intermediates," ed by R. A. Abramovitch, Plenum, New York (1983), Vol. 3, Chapter 5. d) P. M. Warner, *Chem. Rev.*, **89**, 1067 (1989). e) W. T. Borden, *Chem. Rev.*, **89**, 1095 (1989). f) R. Keese and W. Luef, *Topics Stereochem.*, **20**, 231 (1991).

28 H. E. Zimmerman, in "Rearrangements in Ground and Excited States," ed by P. de Mayo, Academic Press, New York (1980), Vol. 3, pp. 131–166.

29 H. H. Jaffé and M. Orchin, "Theory and Applications of Ultraviolet Spectroscopy," Wiley, New York (1962), Chap. 15.

30 a) W. Reppe, O. Schlichting, K. Klager, and T. Toepel, *Liebigs Ann. Chem.*, **560**, 1 (1948). b) A. Cope and W. J. Bailey, *J. Am. Chem. Soc.*, **70**, 2305 (1948).

31 For π-bond shifting in cyclooctatetraenes, see: a) L. A. Paquette, *Acc. Chem. Res.*, **26**, 57 (1993) and references cited therein. b) D. A. Hrovat and W. T. Borden, *J. Am. Chem. Soc.*, **114**, 5879 (1992).

32 According to recent theoretical calculations, the energy required for π-bond shifting in planar D_{4h}-cyclooctatetraene (COT) is 3–4 kcal mol^{-1} which is in good agreement with the measured differences between the energies required for π-bond shifting and ring inversion in monosubstituted derivatives of COT.[31b]

33 T. Tsuji, unpublished results.

34 The distortion angles given in Fig. 5 are dihedral angles and not the actual pyramidalization angles.

35 R. C. Haddon, *Acc. Chem. Res.*, **21**, 243 (1988).

36 M. Okuyama and T. Tsuji, *Angew. Chem., Int. Ed. Engl.*, **36**, 1085 (1997).

37 M. Okuyama and T. Tsuji, unpublished results.

38 a) A. Guijarro and M. Yus, *Tetrahedron*, **51**, 231 (1995). b) H. J. Reich, I. L. Reich, K. E. Yelm, J. E. Holladay, and D. Gschneidner, *J. Am. Chem. Soc.*, **115**, 6625 (1993).

39 K. Wolinski, J. F. Hinton, and P. Pulay, *J. Am. Chem. Soc.*, **112**, 8251 (1990).

40 a) P. v. R. Schleyer and H. Jiao, *Pure Appl. Chem.*, **68**, 209 (1996). b) This criterion was first proposed by Dauben et al: H. J. Dauben, Jr., J. D. Wilson, and J. L. Laity, *J. Am. Chem. Soc.*, **90**, 811 (1968); *J. Am. Chem. Soc.*, **91**, 1991 (1969).

41 a) P. v. R. Schleyer, C. Maerker, A. Dransfeld, H. Jiao, and N. J. R. van Eikema Hommes, *J. Am. Chem. Soc.*, **118**, 6317 (1996). b) G. Subramanian, P. v. R. Schleyer, and H. Jiao, *Angew. Chem., Int. Ed. Engl.*, **35**, 2638 (1996).

42 T. A. Keith and R. F. W. Bader, *Chem. Phys. Lett.*, **194**, 1 (1992); *Chem. Phys. Lett.*, **210**, 223 (1993).

43 D. V. Simion and T. S. Sorensen, *J. Am. Chem. Soc.*, **118**, 7345 (1996).

44 M. Nendel, K. N. Houk, L. M. Tolbert, E. Vogel, H. Jiao, and P. v. R. Schleyer, *Angew. Chem., Int. Ed. Engl.*, **36**, 748 (1997).

45 a) B. A. Hess, Jr. and L. J. Schaad, *J. Am. Chem. Soc.*, **105**, 7500 (1983). b) H. Jiao, N. J. R. van Eikema Hommes, P. v. R. Schleyer, and A. de Meijere, *J. Org. Chem.*, **61**, 2826 (1996). c) H. Jiao, P. v. R. Schleyer, B. R. Beno, K. N. Houk, and R. Warmuth, *Angew. Chem., Int. Ed. Engl.*, **36**, 2761 (1997).

46 The benzene form **49** is predicted to lie higher in energy than the Dewar form **48** by ca. 14 kcal/mol at both the MP2/6-31G* and B3LYP/6-31G* levels.[17]

47 M. Regitz, H. Heydt, and U. Bergsträβer, in "Advances in Strain in Organic Chemistry," ed by B. Halton, JAI Press, Greenwich, Ct. (1996), Vol. 5, pp. 161–243.

48 The [5]paracyclophanes so far prepared are stable only below room temperature in dilute solution in the absence of air and they lack sufficient stability to be isolated.[5]

49 J. J. McCullough, *Chem. Rev.*, **87**, 811 (1987).

50 H. Hopf and F. T. Lenich, *Chem. Ber.*, **107**, 1891 (1974).

51 a) K. Lonsdale, H. J. Milledge, and K. W. Krishna Rao, *Proc. R. Soc., Ser. A*, **255**, 82 (1960). b) H. Hope, J. Bernstein, and K. N. Trueblood, *Acta Crystallogr., Sect. B*, **28**, 1733 (1972).

52 P. O'Neill and A. P. Hegarty, *J. Org. Chem.*, **52**, 2113 (1987). *J. Chem. Soc., Chem. Commun.*, **1987**, 744.

53 A. L. Cossey, L. Lombardo, and L. N. Mander, *Tetrahedron*, **21**, 4383 (1980). b) L. Lombardo and L. N. Mander, *J. Org. Chem.*, **48**, 2298 (1983).

54 H. J. Reich and J. R. Renga, *J. Org. Chem.*, **40**, 3313 (1975).

55 N. C. Yang, M. Chen, and P. Chen, *J. Am. Chem. Soc.*, **106**, 7310 (1984).

56 H. Gan, J. L. King, and N. C. Yang, *Tetrahedron Lett.*, **30**, 1205 (1989).

57 The calculated heat of reaction for the isomerization of **73a** to **59a** is −26.2 kcal mol^{-1}, while that for the fission of parent *p,p′*-dibenzene to two molecules of benzene is −78.4 kcal mol^{-1} (B3LYP/6-31G*).

58 A. Bondi, *J. Phys. Chem.*, **68**, 441 (1964).

59 There exists some ambiguity concerning the bending angles α and β since the nonbridgehead carbon atoms are displaced from the mean plane by 0.004–0.011 Å and the plane of the methylene bridge is not exactly orthogonal to that formed by the bridgehead and the adjacent aromatic carbon atoms.

60 The largest deformation angle ($\alpha + \beta$) previously observed for a paracyclophane, to our knowledge, was 44.6° for a [6]paracyclophane-3-ene derivative: Y. Tobe, K.-I. Ueda, T. Kaneda, K. Kakiuchi, Y. Odaira, Y. Kai, and N. Kasai, *J. Am. Chem. Soc.*, **109**, 1136 (1987).

61 J. C. Barns, J. D. Paton, J. R. Damewood, Jr., and K.

Mislow, *J. Org. Chem.*, **46**, 4975 (1981).

62 a) B. K. Selinger and M. Stern, *J. Chem. Soc., Chem. Commun.*, **1969**, 978. b) D. A. Dougherty, W. D. Hounshell, H. B. Schlegel, R. A. Bell, and K. Mislow, *Tetrahedron Lett.*, **1976**, 3479. c) M. Kimura, H. Okamoto, and S. Kashino, *Bull. Chem. Soc. Jpn.*, **67**, 2203 (1994). d) T. R. Battersby, P. Gantzel, K. K. Baldridge, and J. S. Siegel, *Tetrahedron Lett.*, **36**, 845 (1995). e) J. Harada, K. Ogawa, and S. Tomoda, *Chem. Lett.*, **1995**, 751.

63 R. Hoffmann, *Acc. Chem. Res.*, **4**, 1 (1971). R. Gleiter, *Angew. Chem., Int. Ed. Engl.*, **13**, 696 (1974). M. N. Paddon-Row, *Acc. Chem. Res.*, **15**, 245 (1982). H.-D. Martin and B. Mayer, *Angew. Chem., Int. Ed. Engl.*, **22**, 283 (1983); R. Gleiter and W. Schäfer, *Acc. Chem. Res.*, **23**, 369 (1990).

64 K. K. Baldridge, T. R. Battersby, R. VernonClark, and J. S. Siegel, *J. Am. Chem. Soc.*, **119**, 7048 (1997).

Takashi Tsuji was born in Osaka in 1939 and received his Ph.D. degree in 1967 from Osaka University under the guidance of the late Prof. I. Moritani. He joined the faculty of Osaka University as an instructor in 1967 and was appointed an associate professor at Hokkaido University in 1971, where he has been a professor of chemistry since 1993. From 1968 to 1970, he worked as a postdoctoral research fellow with Prof. E. M. Kosower at the State University of New York at Stony Brook. His research interests are in the chemistry of unsaturated polycyclic compunds including strained molecules, cyclophanes, macrocycles, and compounds related to supramolecular chemistry. He received the Divisional Award of the Chemical Society of Japan in 1999.

Masakazu Ohkita was born in Sapporo in 1962. He completed his undergraduate study in 1985 and received his Ph.D. degree in 1990 under the guidance of Profs. S. Nishida and T. Tsuji from Hokkaido University. He was given a Research Fellowship for Young Scientists from the Japan Society for the Promotion of Science (1989–1990). He has been a research associate at Hokkaido University since 1990. He also worked as a visiting research associate in the group of Prof. J.-M. Lehn at Université Louis Pasteur, Strasbourg, France (1997–1998). His research interests are in organic chemistry, supramolecular chemistry, and materials science.

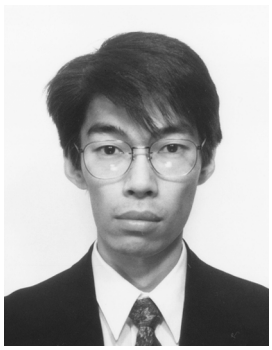

Hidetoshi Kawai was born in Sapporo in 1972. He has been a research associate at Hokkaido University since 2000. He received his B. Sc. (1995) and M. Sc. degrees (1997), under the direction of Prof. T. Tsuji, from Hokkaido University and was given a Research Fellowship for Young Scientists from Japan Society for the Promotion of Science (1998–1999). He received his Ph.D. degree in 2000 from Hokkaido University. His research interests include highly strained molecules, self-assembly and molecular recognition based on hydrogen bonding and aromatic interactions.